Technological reconstruction of the late prehistoric primary copper production of the Vilabouly Complex (central Laos)

Mélissa Cadet, T. O. Pryce, Philippe Dillmann, Thongsa Sayavongkhamdy, Viengkeo Souksavatdy, Thonglith Luangkhoth, Nigel Chang

Technological reconstruction of the late prehistoric primary copper production of the Vilabouly Complex (central Laos)

Mélissa Cadet1 · T. O. Pryce2 · Philippe Dillmann2 · Thongsa Sayavongkhamdy3 · Viengkeo Souksavatdy3 · Thonglith Luangkhoth3 · Nigel Chang4

Introduction

Laos is a mountainous land-locked nation, located at a historical crossroads of cultural influences in northern Mainland Southeast Asia (MSEA). Laos' territory also hosts extensive mineral resources, which leads us to believe it was long a place of exchange and interaction, along routes yet to be defined. Very few late prehistoric Lao sites (Fig. 1) have been discovered, which might allow us to address these issues (Karlström and Källen 1997; White et al. 2009; Pryce 2013; O'Reilly et al. 2019). Indeed, Laos is largely a blank on the regional map before the kingdom of Lan Xang in the fourteenth century (Lorrillard 2014), while developed Southeast Asian states are known, e.g. Champa and Funan in Cambodia/Vietnam, from the end of the Iron Age, up to 1300 years earlier (Malleret 1959; Glover and Yamagata 1995; Stark 1998, 2015; Bourdonneau 2003, 2005; Manguin 2009).

From 2008, SEALIP (the Southeast Asian Lead Isotope Project) began revealing early regional copper/bronze exchange networks, which initially focused on the two known production loci: Phu Lon (PL) in northern Thailand (Pigott and Natapintu 1996; Vernon 1996; Pigott and Weisgerber 1998; Pigott 2019) and the Khao Wong Prachan Valley (KWPV) (Bennett 1988a; Pigott 2019; Pigott et al. 1997; Pryce et al. 2010; Rostoker et al. 1989) in Central Thailand. However, with the discovery of a major copper production centre in Laos, known as the Vilabouly Complex (VC), it transpired most prehistoric regional consumption signatures were far more compatible with the VC than PL and the KWPV (Pryce et al. 2011, 2014). Indeed, the VC's signature has been detected in Bronze Age artefacts as far as central Myanmar (Pryce et al. 2018), showing the potential importance of Laos in late prehistoric exchange networks (Cadet et al. 2019). However, it is necessary to better understand the historical context of Lao copper production, from its epicentre rather than just its extent.

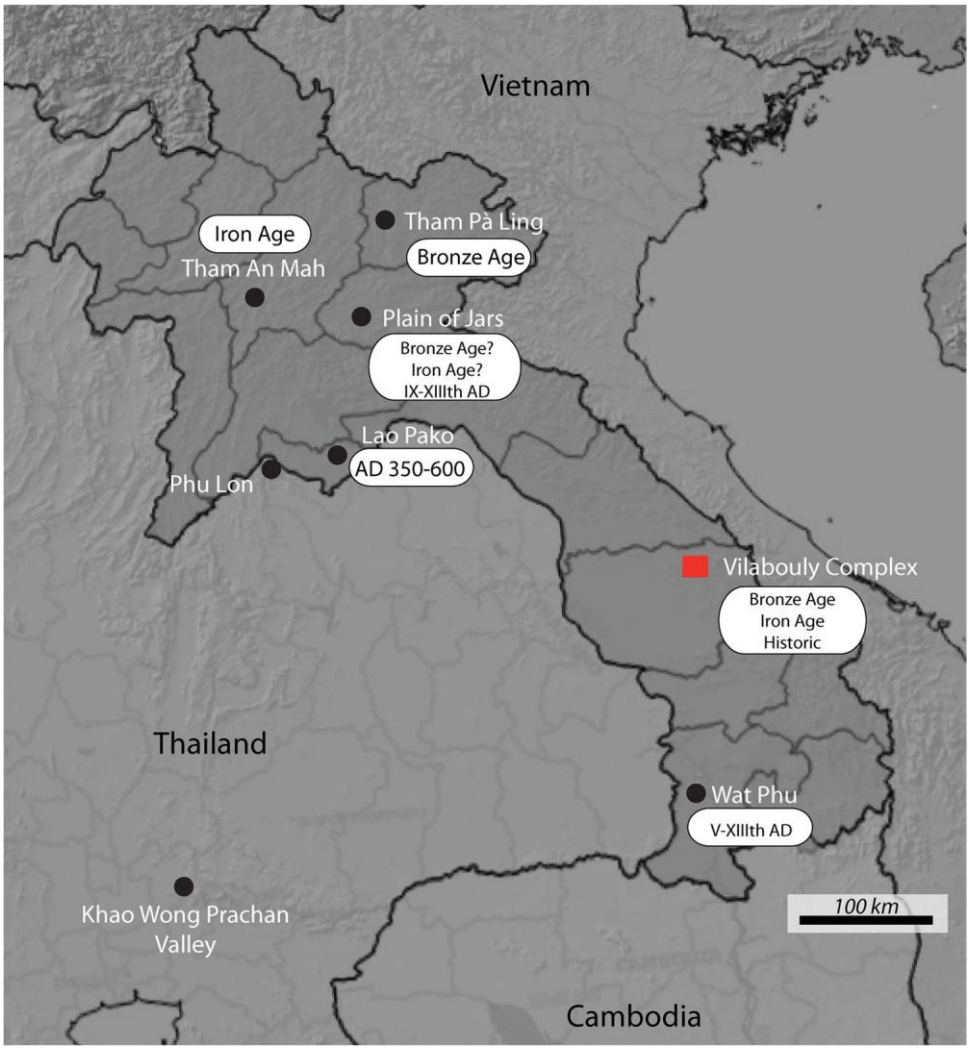

Figure 1 : Map of localization of the Vilabouly Complex and other late prehistoric sites currently known in Laos (Courtesy of ArcGIS)

The VC primary copper production centre was active during the Iron and, probably, Bronze Ages. It is therefore a privileged and unique witness to the potential contribution of the present-day Lao territory to the technological, economic and cultural development of the region. Despite the VC's discovery in the mid-2000s (Tucci et al. 2014) and its likely importance in the exchange networks, no comprehensive archaeometallurgical study had been carried out prior to 2018. By investigating VC copper metallurgy in the round, the aim of the present research was to elucidate the development of metallurgical behaviours in this region of Laos and potential technological transfers from other metalproducing communities, as well as their wider implications at the supra-regional scale for knowledge of protohistoric societies. This would place Laos, for the first time on the map of protohistoric MSEA. This paper will focus on our technological approach with results and interpretations of the archaeometric study of the various artefacts discovered in connection with the production of copper (ores, technical ceramics and slags), alongside the metal evidence, previously published (Cadet et al. 2019). The main issues addressed during this article are the different stages of production, the characteristics of the products/by-products and the type of ores used at Vilabouly.

Geological background

The Vilabouly Complex is situated in the Sepon Mineral District (SMD) of gold and copper deposits, under license to Lane Xang Minerals Limited (LXML), along the southern boundary of the NW-trending Truong Son fold belt in Savannakhet Province, south central Laos. The Sepon Basin is a small scale clastic-carbonate sedimentary basin approximately 20-km long by 8-km wide, belonging to a group of Palaeozoic successor basins (Cromie et al. 2018). The prospect is located at an altitude of around 300 m above sea level, with the central section of the district located longitude 105.59°E and latitude 16.58°N (Cromie 2010). Sepon Mineral District (SMD) stratigraphy comprises Devonian to Carboniferous aged continental fluvial and shallow to deep marine sediments (Sillitoe 1998; Manini et al. 2001; Cromie 2010). At least three mineralization styles are recognized: sedimentary rock-hosted Au, Cu-Au skarn and quartz stockwork porphyry Cu-Mo. Three types of intrusions occur: rhyodacite-porphyry, stocks and dykes.
The two main archaeological sites of the Vilabouly Complex, Thong Na Nguak (also known as Dragon Field) and Puen Baolo are associated with the two main copper exploitation areas of the district, Khanong and Thengkham. At least three main copper mineralization groups are identified: supergene, exotic and hypogene. The main copper minerals are contained in the supergene zone: malachite ($Cu_2CO_3(OH)_2$) and chalcocite (Cu_2S). The chalcocite ores tend to be formed above the primary copper ores (chalcopyrite $CuFeS_2$ and pyrite FeS_2 mainly). Exotic mineralization corresponds to oxidic copper ores containing manganese. The supergene zones have thicknesses between 20and 100-m deep in all the SMD. The main host rocks containing copper minerals are identified as skarn and limestones, as well as porphyries and black carbonaceous shale. Fairly high levels of secondary groundwater-remobilized barite ($BaSO_4$) are identified in the SMD, often associated with malachite (Cromie 2010; Cromie et al. 2018).

Archaeology

Rescue archaeology at LXML started in 2008 under the codirection of Thongsa Sayavongkhamdy, Viengkeo Souksavatdy and Nigel Chang as a collaboration between the Lao Department of National Heritage, James Cook University and the mining concession (Oxiana, followed by OzMinerals and then MMG-LXML). Archaeological finds in the Vilabouly Complex show a long occupation period, thought to be from the Neolithic with a concentration of Metal Age copper mining sites with associated occupation and funerary activity, as well as isolated finds from the Lan Xang Kingdom (AD 1354–1707) and remains from the mid-twentieth century Indo-China wars (Tucci et al. 2014). VC extraction seems to be active since the Bronze Age, as evidenced by lead isotopic exchange results (Pryce 2019; Pryce and Cadet 2018; Pryce et al. 2016), material culture and dating on mining shaft materials.

Mining areas

Five archaeological sites identified here correspond to ancient mining extraction places: Khanong A2, Thengkham South C, Thengkham South D, Thengkham East and Phabing B (Fig. 2). The mining places were first identified by the discovery of ancient mining shafts with preserved organic matting structures (wood and bamboo), some extending 40-m deep (Tucci et al. 2014). Direct dates from ancient mining shaft structural elements suggest copper mining between about BC 1000 and AD 700 (Chang 2016). The mining shafts represent the

depth at which the major supergene mineralization occurs, as they range from 20to 100-m deep. The Khanong vertical shafts extend into the supergene zone of copper deposits where 99% malachite is found (compared to other species). The remaining 1% corresponds to azurite and cupro-allophane traces containing manganese clay (M. Stott, *pers. comm*.).

Figure 2 : Location of the archaeological sites of the Vilabouly Complex (courtesy of Google Earth)

Ore processing places

Two archaeological sites correspond to ancient ore processing places (Fig. 2) dating from the regional Iron Age and potentially Bronze Age: Puen Baolo and Thong Na Nguak.

Puen Baolo or Crucible Terrace ('PBL') was the first site to be excavated, alongside Thong Na Nguak. It was the subject of major excavation seasons from 2008 to 2015, with modern mining activity redirected to other parts of the mining tenement during these years (leading to the discovery of the other sites already mentioned). The nine excavation seasons exposed 1120 m2, showing mining and production activities with shafts, slags, crucibles, ores and metal artefacts. Commercial mining activity restarted here in 2016, leading to the discovery of an adjacent, extensive, field (Thengkham South C) of ancient mining shafts reflecting similar technology as seen at Khanong A2, Thengkham South D and Thengkham East. PBL appears to be an occupation and processing site, located on a small terrace.

On the PBL portion of the site we see a natural substrate of clay and soft siltstone, overlain by a layer of occupation and ore processing debris. Varying concentrations of metallurgical production debris (slag, technical ceramic and mineral) were found, some of which were quite dense. A wide variety of pits with different characteristics and dimensions were also discovered. Many of these pits were associated with ash, showing their potential use during a metallurgical process step or domestic activities. The pits have diameters between 40 and 80 cm, with round and oblong shapes identified. Some are relatively shallow, about 30 cm, while others are deeper, with depths up to 1 m. Most of the pits uncovered at Puen Baolo were surrounded with fragmentary slags and crucibles. These different structures may represent temporal and technical evolutions, but the disturbed archaeological deposits of Puen Baolo do not allow us to establish definite stratigraphic sequencing in most instances. However, burials and other features cut into the natural substrate are thought to date to the Bronze Age (regionally, c. 1000 BC to c. 400 BC) based on associated artefacts, superposition by industrial detritus and likely ritual or burial deposits associated with the Iron Age. The

bulk of the complete bronze/copper alloy artefacts is associated with these deeper features — in particular bowtie ingots — along with chalcedony beads and specific pottery types. Iron and glass are not found in these features, but iron artefacts do occur in upper levels. It should be noted that the acidic soils have probably dissolved any original bone in the burial features (Chang 2016). A second type of burial or deliberate artefact cache has been identified. These lie within the upper layers of deposit and include iron axes, conical copper ingots and pottery. Surprisingly, no glass has been found at this site; glass is usually an Iron Age marker for MSEA. One radiocarbon date from the upper edge of a pit or mining shaft places this later Puen Baolo activity to at least the regional early Iron Age (361–202 BC).
The opening of the Thengkham South C pit allowed dating of the PBL-associated mining shafts. As with all the mine shaft dates, we have relied on samples of structural rattan or bamboo preserved in permanently wet clays 10 m or more below the ground surface, with the earliest determination of approximately 1000 BC (1071–922 BC). Other shaft dates confirm that mining activity continued at PBL/TKS-C to at least as late as approximately AD 700 (AD 660–767).
Thong Na Nguak or Dragon Field ('TNN') was excavated for one season in 2008 at around 10 km from PBL, with the aim of confirming that in situ archaeological evidence was indeed present at the site. With this confirmed, all activity on the site ceased due to its spiritual importance for local communities. A single radiocarbon date places it in the Early Iron Age (346–54 BC, in a burial jar). The burial jar was associated with three others, within one of many rectangular stone arrangements, along with other finds indicating hightemperature ore processing with slags, crucibles, ores and metal artefacts. The dated burial jar was sealed by a large rock, completely covering the mouth of the jar and contained (as well as the charcoal used for dating) a unique set of dark and pale blue glass beads, along with a single orange bead. The latter particularly characteristic of the early to mid-Iron Age in MSEA.

Assemblage

The archaeological material selected for analyses comes from Puen Baolo and Thong Na Nguak, and are classified as follows: minerals, slags, technical ceramic fragments and copper-alloy objects, the latter published in 2019 (Cadet et al. 2019). The corpus was selected in November 2017 at the LXML facility in Laos, using a stratigraphic and sequential approach. The selection was also made by type of artefacts (slags, crucibles, ores, copper-base objects) previously identified (Table 1). Our attention has also focused on the least disturbed archaeological areas, in order to have the most representative sequences possible. The total weight of material recorded is of 142 kg (which represents the major part of the available material in storage), quite low compared to the Khao Wong Prachan Valley in Thailand. However, it should be noted that not all materials discovered during the excavations were collected, with what the excavators considered a representative sample kept due to storage and processing limitations. Most of the selected archaeological material comes from PBL because the site was more extensively excavated (ten seasons) than TNN (one season). We must also take into consideration the potential bias in the results that maybe expressed by this difference in material quantity between the two sites.
Thirteen samples of minerals from Puen Baolo and two from Thong Na Nguak were selected, from a small pool of potentials (Fig. 3). A large part of the corpus consists of technical ceramics, some of which can be attributed to use during a high temperature stage, via various characteristics that will be described below. Most of these ceramics seem to be

crucibles; 28 fragments of technical ceramics attributed to crucibles (Fig. 4) were selected for study, 22 for PBL and 6 for TNN.

Table 1 : Artefacts selected for analyses with their associated context

Sample	Square	Layer	Split	Context	Type	Weight (g)	Length (cm)	Thikness (cm)
G15_2_1_7305	G15	2	1	7305	Copper ore	3		
E15_2_3_3282	E15	2	3	3282	Copper ore	2		
E15_2_2_3218	E15	2	2	3218	Copper ore	51,5		
E15_3_1_3278_e	E15	3	1	3278	Copper ore	5		
C17_3_1_a	C17	3	1		Copper ore	4		
C17_3_1_b	C17	3	1			34,5		
B17_2_2_3311	B17	2	2	3311	Copper ore	2		
C16_3_2_3523	C16	3	2	3523	Copper ore	3		
S9_1_2_5503	S9	1	2	5503	Copper ore	18		
G15_3_3_7311_b	G15	3	3	7311	Iron ore	8,5		
E15_3_3_4040	E15	3	3	4040	Iron ore	3		
B14_2_4_7005	B14	2	4	7005	Iron ore	40		
DD14_2_2_7126_7113	DD14	2	2	7126	Iron ore	127		
DF_1-A_B1_53	DF	1-A	B1	53	Copper ore	2,5		
DF_1-A_4_152	DF	1-A	4	152	Copper ore	4		
G15_3_1_7309_7303_b	G15	3	1	7309	Crucible	20	5,5	1,5
G15_3_3_7311_c	G15	3	3	7311	Crucible	10	3,5	1
G15_3_4_7316_d	G15	3	4	7316	Crucible	37	7	1 to 1,5
E15_3225_a	E15			3225	Crucible	18	3,5	2
E15_2_1_3211	E15	2	1	3211	Crucible	57	3,5	4
C17_3_2_3119	C17	3	2	3119	Crucible	14	4,5	1,5 to 2
C17_1_2_b	C17	1	2		Crucible	5	3	1
B14_1_1_7001_a	B14	1	1	7001	Crucible	19	3	1,5
A15_4_1_6709_b	A15	4	1	6709	Crucible	4	2	1
A15_3_1_6703	A15	3	1	6703	Crucible	15	4	1,5
AA15_2_2_6803_a	AA15	2	2	6803	Crucible	11	3	2
C14_2_1_7209_a	C14	2	1	7209	Crucible		3	2
C14_1_4_7205	C14	1	4	7205	Crucible	42	6	1 to 2
C14_2_3_7217	C14	2	3	7217	Crucible	12	3	0,5
B17_2_1_3303_h	B17	2	1	3303	Crucible	34	3,75	1,5 to 2
B17_2_2_3314_a	B17	2	2	3314	Crucible	37	6	1 to 2
B17_2_2_3303_f	B18	2	2	3303	Crucible		2,4	
C16_3_1_3529	C16	3	1	3529	Crucible	50	6	1 to 3
DD14_2_1_7123_a	DD14	2	1	7123	Crucible	12	1	1
D13_2_1_3706_a	D13	2	1	3706	Crucible	105	8,5	1 to 2,5
D13_2_1_3706_b	D13	2	1	3706	Crucible	28	4,75	0,5 to 2
S9_1_1_5503_c	S9	1	1	5503	Crucible	4	2	0,5
WEST1_2_3_a	WEST1	2	3		Crucible	68	4	1 to 2,5

DF_1-B_3_113	DF	1-B	3	113	Crucible	26	6	1,5 to 2
DF_1-A_B3_90	DF	1-A	B3	90	Crucible	7	1	1
DF_1-C_2	DF	1-C	2		Crucible	10	1,5	1
DF_1-E_3_37	DF	1-E	3	37	Crucible	10	1	1
DF_1-A_4_131	DF	1-A	4	131	Crucible	20	4	1 to 2
DF_1-A_4_131_b	DF	1-A	4	131	Crucible	10	1,5	0,5 to 1
B17_2_1_3303_g	B17	2	1	3303	Scorched clay			
C17_2_1_3112	C17	2	1	3112	Scorched clay			
E13_clay lining	E13				Scorched clay			
DD14_1_1_7108	DD14	1	1	7108	Scorched clay			
A5_159_367	A5			159-367	Scorched clay			
A15_3_1_6705_a	A15	3		6705	Slag	25	3,4	1,2
AA15_2_2_6803_b	AA15	2		6803	Slag	2	2,5	0,3
AA15_2_3_6811_b	AA15	2		6811	Slag	20	3	0,6
AA15_3_1_6808_b	AA15	3		6808	Slag	10	1,7	1,3
AA15_3_1_6808_d	AA15	3		6808	Slag	10	1,9	0,7
AA15_3_1_6808_e	AA15	3		6808	Slag	5	2,3	0,3
B14_1_1_7001_c	B14	1		7001	Slag	4	1,8	0,3
B14_1_2_7002_b	B14	1		7002	Slag	14	3,5	0,6
B17_1_1_3301_b	B17	1		3301	Slag	22	3	1,2
B17_2_1_3303_d	B17	2		3303	Slag	2	1,8	0,3
B17_2_1_3303_i	B17	2		3303	Slag	11	3,5	0,4
B17_3_1_3312_c	B17	3		3312	Slag	1	1,9	1
C14_1_4_7205_a	C14	1		7205	Slag	18	3,5	2
C14_1_4_7205_c	C14	1		7205	Slag	4	2,5	0,5
C14_2_1_7209_b	C14	2		7209	Slag	8	2,2	0,6
C14_2_3_7219_a	C14	2		7219	Slag	7	2,8	0,7
C14_2_3_7219_c	C14	2		7219	Slag	3	2,2	0,2
C16_3503_a	C16			3503	Slag	45	4,5	0,7
C16_3503_b	C16			3503	Slag	8	2,5	0,3
C16_GENSPIT_3501_a	C16			3501	Slag	7	2,7	0,2
C17_1_1_3117_a	C17	1		3117	Slag	55	5,5	0,9
C17_1_1_3117_b	C17	1		3117	Slag	10	2,5	1
C17_1_1_3117_c	C17	1		3117	Slag	10	5	2
C17_1_2_a	C17	1			Slag	80	4,5	2
C17_1_2_d	C17	1			Slag	8	2,5	0,4
C17_2_1_3107_b	C17	2		3107	Slag	72	4,7	0,5
C17_2_1_3107_e	C17	2		3107	Slag	2	1,5	1
CC14_3_7116_a	CC14	3		7116	Slag	12	3,2	0,4
CC14_3_7116_c	CC14	3		7116	Slag	35	3	1,8
CC14_3_7116_g	CC14	3		7116	Slag	3	2	0,8
D10_1_1_2004	D10	1		2004	Slag	118	5,5	2,9
D13_3729_1709	D13			3729	Slag	76	4,8	2,6
E15_2_2_3218_b	E15	2		3218	Slag	8	2,5	1,4
E15_2_2_3218_c	E15	2		3218	Slag	11	2,3	1,5
E15_2_2_3218_e	E15	2		3218	Slag	12	3	0,4

E15_3_1_3277_b	E15	3		3277	Slag	2	2	0,7
G15_1_3_7304_c	G15	1		7304	Slag	45	4,5	0,6
G15_2_2_7305_b	G15	2		7305	Slag	3	2,9	0,4
G15_2_2_7305_h	G15	2		7305	Slag	12	3	1,2
G15_3_1_7309_a	G15	3		7309	Slag	6	2,5	0,2
G15_3_4_7316_7309	G15	3		7316	Slag	75	7,7	1,5
S9_2_2_5505_b	S9	2		5505	Slag	4	1,5	1,3
S9_2_2_5508	S9	2		5508	Slag	4	2,5	1,5
DF_1_2_2_43	DF				Slag	10	2,5	1,2
DF_1_A_2_40	DF				Slag	4	2	1,2
DF_1_A_4_165_b	DF				Slag	28	3	1,7
DF_1_A_4_133	DF				Slag	3	1,4	0,3
DF_1_A_4_165_a	DF				Slag	15	4	1,3
DF_1_A_138_a	DF				Slag	31	3	2,5
DF_1_A_138_b	DF				Slag	3	2,5	1
DF_1_B_2_42	DF				Slag	28	3,5	1,6
DF_1_B_3_93_a	DF				Slag	5	2,6	0,3
DF_1_B_3_93_b	DF				Slag	5	2	1
DF_1_C_3_8_c	DF				Slag	4	2	1,5
DF_1_D_3_99	DF				Slag	34	3,5	2,3
DF_1_E_2_39	DF				Slag	1	1,5	0,2
SEALIP_LA_PBL_42	F15	2	3	5416	Multi-layer artefact	129	6,5	
SEALIP_LA_PBL_48	B17	2	1	3303	Multi-layer artefact	65	4,5	1,7
SEALIP_LA_PBL_49	C15	3	1	2423	Multi-layer artefact	32	4,3	0,8
SEALIP_LA_PBL_50	C15	3	1	2423	Multi-layer artefact	46	4,5	1,6
SEALIP_LA_PBL_51	C15	3	1	2423	Multi-layer artefact	34	4,6	1,7
SEALIP_LA_PBL_52	E4	2	2	5006	Multi-layer artefact	84	4	1,5
BB14_3_3_7113	BB14	3	3	7113	Multi-layer artefact	23	3,5	1

After the technical ceramics, most of the Puen Baolo and Thong Na Nguak corpus consists of fragments of slag selected after a visual examination, in order to incorporate the three types identified: flat, massive and coarse (Fig. 5) defined by their macroscopic characteristics. The flat slags are often described for the European Bronze Age (Herdits 2003; Burger 2008; Bourgarit et al. 2010) and correspond to slag of low thickness (0.3–1 cm), homogeneous and dense. The massive slags have the same characteristics as the flat slags except for their thickness (> 0.8 cm). This type of slags has been described for the Italian Bronze Age (Addis et al. 2016, 2017). The coarse slags correspond to slags that have irregular shapes and are sometimes porous with variable dimensions and thicknesses. In total, 137 slag fragments were selected (additional data are given in Online Resource 1), 122 for Puen Baolo and 15 for Thong Na Nguak (but only 56 for OM/SEM–EDS analyses, Table 1). They represent a mass of about 1 kg, which is, we note, very low.

Another part of the corpus is composed of seven samples, originally thought to be ingots (or slag ingots) but now recognized as intermediary products (now named ‘multi-layered artefacts’ after to distinguish them from the ingots), with a round/ conical shape and a layered structure visible to the naked eye (Fig. 6). The layered structure was formed by the density differences between the three products identified in these artefacts (metallic copper, matte and slag).

Methodology

The artefacts were all submitted to macroscopic observations, photographed, weighed and measured. Cut samples were mounted in epoxy resin and ground using silicon carbide wet-dry paper (80–4000 grit), before polishing with diamond pastes (3 and 1 µm) under water.

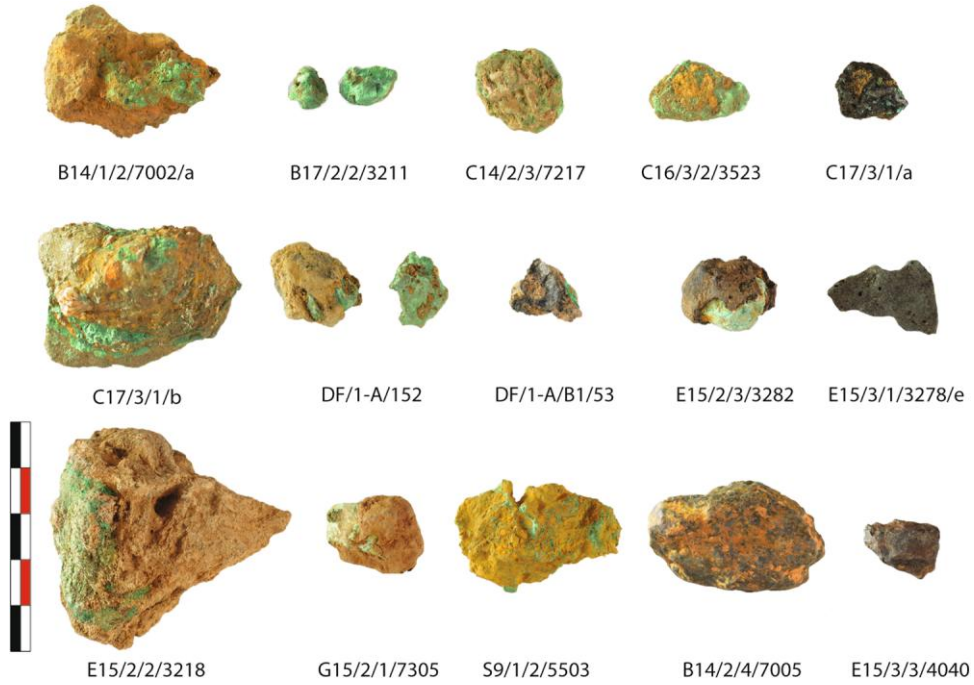

Figure 3 : Examples of copper and iron minerals from Vilabouly

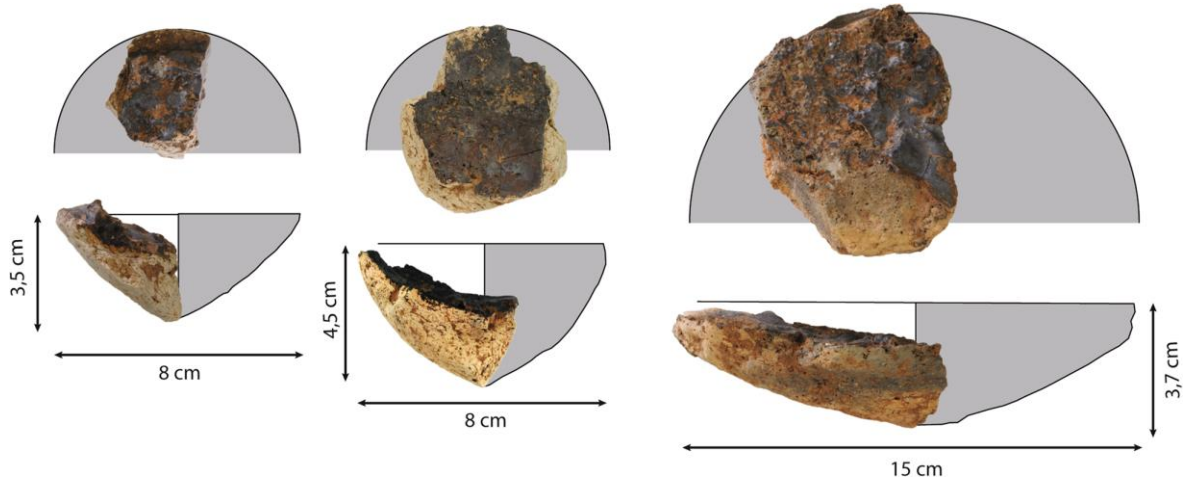

Figure 4 : Examples of archaeological crucibles from Vilabouly

Figure 5 : Examples of archaeological slags discovered at Vilabouly

Identification of trace elements was conducted at the *Service d'Analyse des Roches et des Minéraux* of the Centre for Petrographic and Geochemical Research (SARM-CRPG) in Nancy, France, on the 137 slag samples and 18 crucible samples, using Optical Emission Spectroscopy (ICP-OES) *Thermo Fischer ICap 6500* for 11 major and minor oxides (SiO_2, Al_2O_3, Fe_2O_3, MnO, MgO, CaO, Na_2O, K_2O, P_2O_5 and TiO_2) and by Inductively Coupled Plasma Mass Spectroscopy (ICP-MS) *Thermo Elemental X7* for 44 trace elements (As, Ba, Be, Bi, Cd, Ce, Co, Cr, Cs, Cu, Dy, Er, Eu, Ga, Gd, Ge, Hf, Ho, In, La, Lu, Mo, Nb, Nd, Ni, Pb, Pr, Rb,Sb,Sm,Sn,Sr,Ta,Tb,Th,Tm,U,V,W,Y,Yb,Znand Zr). Sulphur content was obtained with an analyzer Carbon–Sulfur *Leco SC 144 DRPC*. Samples were prepared and analyzed following the methodology described by Carignan et al. (2001). The bulk analyses result for the slags were used for a sub-sampling (56 samples) for OM and SEM–EDS.

The microstructures were studied by Optical Microscopy (OM) on the polished samples with a *Zeiss Imager A2 vario Axio* microscope. The OM samples were then carbon coated for Scanning Electron Microscope (SEM, JEOL 7001F) observation coupled to Energy Dispersive Spectrometry (EDS) analyses in order to identify different phases and inclusions. The SEM–EDS was operated in both secondary electron (SE) and backscattered electron (BSE) modes, using a 20-kV accelerating voltage, a 10-mm working distance with an Oxford Silicon Drift Detector, and processed using *Oxford Instruments Aztec* software. Detection limit was estimated at 0.5 wt%, with a count rate of 4000/s (detection time of 40 s) to provide clear resolution of pertinent peaks with respect to background noise.

Figure 6 : Examples of multi-layered artefacts from Puen Baolo. To the right, the cut samples showing the different layers

We consider that the relative quantification error (2 σ) is about 10% of the measured value. Global composition for each sample was obtained by average of 3 to 4 areas scan per sample.

The mineral samples were also analyzed by X-ray diffraction (XRD) in order to identify the type of ore. XRD analyses were done on powders with an X-ray generator of rotating anode *RU-200B* (*Rigaku*). XRD data are collected using two detectors: a pixel hybrid detector *Pilatus 300 K* (*Dectris*) and a 2D 'Image Plate' detector (*Fuji*). 2D images were integrated in a circular manner with *Fit2D* software (Hammersley et al. 1996) and the phase identification was done using *Diffrac-EVA* (*Bruker*) integrating an ICDD database and the 'Crystallography Open Database' (Grazulis et al. 2009).

Results

Ores

Two categories of minerals have been defined, by their appearance, phases and composition in the OM, SEM–EDS and XRD. The first group consists of twelve carbonate and oxidic copper ores. They are mainly associated to malachite (Cu2CO3(OH)2), a copper carbonate. For some samples, malachite is associated with other minerals, mainly quartz (SiO2), but also goethite (α-FeOOH) which is a minor phase, as well as another copper oxide, cuprite (Cu2O). A black ore fragment of the corpus consists of iron and copper oxide, delafossite (CuFeO2) as well as malachite. This latter sample (PBL_E15_3_1_3278_e) could also be a piece of slag resulting from oxidizing conditions. The second group consists of three iron minerals, goethite (α-FeOOH) and haematite (α-Fe2O3) oxides associated with quartz (Table 2).

Technical ceramics

The crucible samples from PBL and TNN are all very fragmentary, which could demonstrate ancient metallurgists were crushing them or that they were disposed on a surface that was trampled. Nevertheless, it was possible for some fragments of PBL to attempt a reconstruction of their original shape/size. As the pieces of Thong Na Nguak were all very

fragmentary and altered by heat and their exposure in the hearth, no attempt to reconstruct their form could be made.
The crucibles have an open and shallow shape with a convex bottom. They have an estimated diameter between 60and150mmandadepthof20to85mm,withanaverage depth of 38 mm. In section, a colour gradient can be seen from the interior to the exterior of the crucible, meaning the heating must have been internal. Moreover, of the fragments of crucibles studied, for which the internal part is preserved, all show slag layers up to 7-mm thick. No differentiation between the crucibles of Puen Baolo and Thong Na Nguak was possible by macroscopic examination.
The crucible paste is composed of a non-calcareous clay (Fig. 7) containing an average composition of silica at 68 wt%, alumina at 22 wt% and iron oxide at 4 wt% (Table 3). The paste contains other minor components: K2O (2.5 wt%), TiO2 (0.8 wt%), MgO (0.7 wt%), P2O5 (0.3 wt%) and CaO (0.5 wt%). Copper alloying elements are identified as traces: Cu (2500 ppm), Pb (160 ppm) and Zn (330 ppm), Sn is detected under 20 ppm (additional data are given in Online Resource 2).
Different types of mineral inclusions can be identified in the crucible paste (Fig. 8). The main mineral inclusion corresponds to quartz grains (SiO2), identified by their shape and composition under SEM–EDS of silica at 48 wt%. In addition to quartz grains, other inorganic inclusions are identified in the crucible paste. First, a titanium oxide, rutile (TiO2). There are two other, more sporadic, types of inclusions, zircon (ZrSiO4), which is identified by its angular to sub-rounded morphology, its brilliant white colour under SEM-BSE and an average zirconium composition of 45 wt% and silica at 16 wt%. The presence of a last, rarer mineral is identified for only six samples. These are potassium feldspars (KAlSi3O8), usually altered by heating. Macroscopic analysis revealed the presence of an organic temper for the majority of samples: it is here identified as rice chaff. The rice chaff has obviously burnt out but characteristic elongated pores retain the original structure (Fig. 8a).
The SEM–EDS analyses (Table 4) of the internal slag layer of the crucibles revealed two types of slag layers (Fig. 7): one corresponding to high FeO and low SiO2 and the second to low FeO, high SiO2 and CuO content. Both types are confirmed by the microstructural observation: the first type corresponds to fayalitic slags and the second to vitreous copper-rich slags (Fig. 8). The main differences are the presence of olivine crystals for the fayalitic slag and a vitreous aspect for the second type of slag with higher copper content. The fayalitic slags are composed on average of FeO (52 wt%), SiO2 (34 wt%) and Al2O3 (7 wt%), containing crystals of fayalite (Fe2SiO4) and magnetite (Fe3O4) in a glassy matrix. Despite the relatively low amount of Cu in this group of slags, metallic copper and copper sulphide inclusions were identified by their morphology and composition, whereas the vitreous slags are composed on average of SiO2 (51 wt%), FeO (19 wt%), Al2O3 (12 wt%) and CuO (9 wt%). The microstructure of these slags is mainly composed of a glassy matrix with iron oxide and metallic copper inclusions. For two samples from Thong Na Nguak (DF_1-A_4_131/a and b), the copper iron oxide delafossite (CuFeO2) is identified by its composition and needle habit, indicating more oxidizing conditions and loss of copper (Fig. 8).

Table 2 : Elemental composition of the mineral samples (SEM–EDS, wt%) and identification of the mineral phase following XRD. < ld. = below detection limit

Sample	O	As	Pb	Zn	Cu	Fe	Mn	Ti	Ca	K	Al	P	Si	Cl	S	Mg
PB_G15_2_1_7305	30,0				69,8								0,2			

PBL_E15_2_3_3282	29,2				55,3	6,8	0,3	0,2	0,1		2,0		5,9	0,1	0,2	0,2
PBL_E15_2_2_3218	38,4	0,2			37,0	0,3							24,2			
PBL_E15_3_1_3278_e	29,8				32,8	15,6	1,1	0,2	0,4	0,3	5,0	0,8	13,6			0,6
PBL_C17_3_1_a	20,8	2,0			63,8	2,9	0,5	0,1	0,2	0,1	1,1		6,5	1,3	0,5	1,4
PBL_C17_3_1_b	40,1				29,8	11,8	0,7	0,1	0,2	0,8	2,8		13,0	0,1	0,1	0,7
PBL_C14_2_3_7217	68,7				29,3				0,3		0,3		1,6			0,2
PBL_B17_2_2_3311	31,3				68,4				0,0				0,2		0,2	
PBL_C16_3_2_3523	39,9			0,2	42,0	18,9	0,7				0,2		1,5	0,1	0,1	0,1
PBL_S9_1_2_5503	47,7				14,3	31,3					0,6		6,0			
PBL_G15_3_3_7311_b	33,3				1,2	64,1			0,2				1,3		0,2	
PBL_E15_3_3_4040	30,9				1,0	65,6					1,1		1,6		0,1	
PBL_B14_2_4_7005	30,2				0,4	65,6	1,0		0,2		1,2		1,6			
DF_1-A_B1_53	53,6				1,2	19,9	0,4		0,3	0,2	1,4	0,4	22,5			
DF_1-A_4_152	54,1				45,4	0,7							0,2			

Slags

Slags

The Vilabouly Complex slags are all fragmentary, generally not exceeding 5 cm in length, though one fragment measures 8 cm. The slags have been separated in three main types based on their macroscopic features (flat, massive, coarse). The bulk composition of the slags (Fig. 9 and Table 5) reveals no compositional variation between these three types of slags. This observation is confirmed by the microstructural observation. The same main crystals are identified for the three types with some variations due to the heterogeneous nature of archaeological slags. The copper content is relatively low with an average composition of 2 wt% CuO for PBL and 3 wt% CuO for TNN.

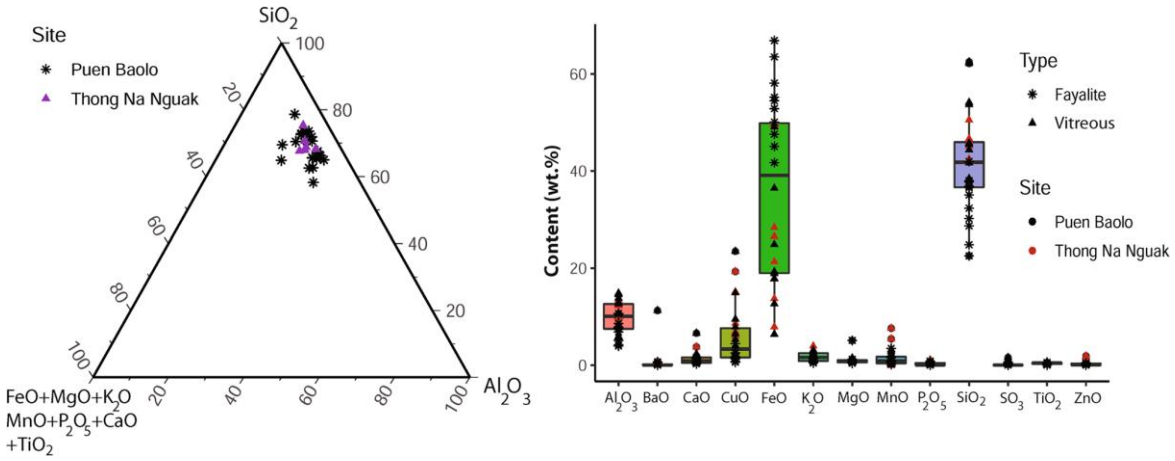

Figure 7 : Left: Ternary diagram with the average composition of the crucible pastes for Puen Baolo and Thong Na Nguak (SEM–EDS, wt%). Right: Boxplot diagram with the composition of the slags

The slags are composed of fayalite crystals, iron oxide mainly magnetite (as suggested by the stoichiometry and the shape) in a glassy matrix along with metallic copper and copper sulphide inclusions (Fig. 10). The magnetite crystals have different habits: band, acicular with predominance of polyhedral crystals (Fig. 10a, b) in a few cases globular wüstite (FeO) is identified. The copper content detected in the bulk composition comes from metallic inclusions that are of two types: precipitated crystals and partially reacted minerals. The inclusions have been separated into three types: metallic copper, secondary sulphide minerals (chalcocite Cu2S, covellite CuS) and primary sulphide minerals (chalcopyrite CuFeS2, bornite Cu5FeS4). The partially reacted minerals correspond mostly to the primary sulphide mineral, chalcopyrite (Fig. 10). Apart from the metallic inclusions, other partially reacted phases can be identified for some slags, mainly quartz grains (SiO2), some barite (BaSO4) and black crystals under the SEM identified as potential leucite (KAlSi2O6). However, compositional and microstructural differences can be observed between PBL and TNN in their MnO and ZnO content which are higher for TNN (Fig. 9). The microstructure described above can be applied to both PBL and TNN except for metallic inclusions. Indeed, for TNN, only two types of metallic inclusions have been recorded: metallic copper and secondary copper sulphide inclusions (Fig. 11). Primary copper sulphide inclusions are absent from TNN slags.
The slag compositions from PBL and TNN have been compared to those for the internal slag layers of the crucibles (Fig. 12). The internal slag layers with a fayalitic composition are comparable to the 'independent' slag (slag not associated to a crucible) whereas the vitreous slag layers from the crucibles have a composition between the fayalitic slags and the crucible walls seeming to be more dependent on reactions with the crucible paste.

Multi-layered artefacts: copper, slag and matte

A last category of artefacts, named multi-layered artefacts, has been defined with seven samples: SEALIP/ LA/PBL/42, SEALIP/LA/PBL/48–52 and PBL/ BB14/3/3/7113 (Fig. 6). These artefacts have a round shape with a diameter between 40 and 65 mm and weight of 32–129 g. The multi-layered artefacts are most likely cast and kept the shape of the mould/depression in which it solidified. Partial sandstone moulds for these forms have been recovered from PBL. In section, the artefacts have a layered structure depending on the density of the different compounds: metallic copper, matte and/or slag (Fig. 13). The matte is an intermediary compound composed of copper, sulphur and/or iron produce when sulfidic ores are present in the smelting charge. It involves a generally more complex process than the use of carbonate/oxidized ores (Cadet et al. 2021). The layers can easily be seen with the naked eye and are confirmed by microstructural and compositional analysis.
The metallic copper is present for four samples (SEALIP/ LA/PBL/48, 50, 51 and 52) and is composed of Cu at 97 wt%, S at 1 wt% and O at 2 wt% (Table 6) The microstructure contains round copper sulphide inclusions composed of Cu (79 wt%), S (19.5 wt%) and traces of Fe.

Table 3 : Chemical composition of the crucible paste (SEM–EDS, wt%). < ld. = below detection limit

Sample	Site	MgO	Al_2O_3	SiO_2	P_2O_5	SO_3	Cl	K_2O	CaO	TiO_2	MnO	FeO	CuO	Sn	Mo	Total

PBL_A15_3_1_	Puen		20,	72			0,	2,	0,	0,		1,	0,		99,
6703	Baolo	0,5	0	,9			4	4	4	9		7	5		8
PBL_A15_4_1_	Puen		21,	69	0,	0,	0,	3,	0,	0,		2,	0,		99,
5709_b	Baolo	0,7	0	,6	3	6	5	3	5	7		3	4		9
PBL_B14_1_1_	Puen		17,	64	0,	0,	0,	3,	0,	0,		11	0,		99,
7001_a	Baolo	0,6	0	,4	5	2	2	4	4	8		,8	3		7
PBL_B17_2_1_	Puen		23,	70	0,			3,	0,	0,		1,	0,		100
3303_f	Baolo	0,7	0	,5	5			0	5	7		2	2		,2
B17_2_2_3314	Puen		22,	71			0,	2,	0,	0,		1,	1,		100
_a	Baolo	0,6	0	,0			2	8	5	7		3	1		,2
PBL_C14_2_3_7	Puen		15,	68	1,			1,	0,	0,		10	1,		99,
217	Baolo	0,4	0	,7	0			8	3	8		,5	1		7
PBL_C17_1_2_	Puen		20,	72				3,	0,	0,		1,	0,	0,	99,
b	Baolo	0,6	0	,5				6	2	7		8	4	6	6
PBL_D13_2_1_	Puen		26,	64	0,	0,		2,	0,	0,		3,	0,		100
3706_b	Baolo	0,8	4	,8	6	5		1	3	9		2	3		,0
PBL_DD14_2_1	Puen		18,	72			0,	3,	0,	0,		3,	0,		100
_7123_a	Baolo	0,7	7	,2			4	4	5	7		1	3		,0
PBL_E15_3225_	Puen		27,	63	0,		0,	1,	0,	0,		2,	2,		100
a	Baolo	0,5	9	,2	7		4	2	3	8		5	5		,0
PBL_S9_1_1_55	Puen		18,	72			0,	1,		1,		3,	0,	0,	99,
03	Baolo	0,7	9	,4			2	7		1		7	6	6	4
PBL_C14_2_1_7	Puen		18,	72	0,	0,		2,	0,	1,		3,	0,	0,	99,
209_a	Baolo	0,8	8	,5	1	1		1	3	1		8	3	2	8
PBL_B17_2_1_	Puen		25,	67	0,		0,	2,	0,	0,			0,		100
3303_h	Baolo	0,7	6	,1	4		3	1	4	7	2,2		4		,0
PBL_AA15_2_2	Puen		14,	78	0,		0,	1,	0,	1,		3,	0,		100
_6803_a	Baolo	0,5	1	,2	3		5	3	4	0		5	09		,0
PBL_G15_3_4_	Puen		26,	62			0,	3,	0,	1,		5,	0,		100
7316_d	Baolo	0,9	9	,5			1	0	3	0	0,1	1	1		,0
PBL_G15_3_1_	Puen		25,	62				2,	0,	0,		7,	0,		100
7309_b	Baolo	0,9	9	,4				5	3	5		2	3		,0
	Puen		26,	65	0,		0,	2,	0,	0,		1,	0,		100
E15_2_1_3211	Baolo	0,8	9	,7	8		3	1	5	7		6	6		,0
	Puen		25,	64				2,	0,	1,		4,	1,		100
WEST_1_2_3	Baolo	0,6	1	,9				8	4	0		1	2		,0
PBL_D13_2_1_	Puen		25,	65				1,	0,	1,		4,	0,		100
3706_a	Baolo	1,0	3	,5				8	4	3		6	2		,0
PBL_G15_3_3_	Puen		29,	58				2,	0,	0,		7,	0,		100
7311_c	Baolo	1,0	1	,0				5	4	7		9	5		,0
PBL_C16_3_1_3	Puen		25,	66	0,		0,	1,	0,	0,		2,	0,		100
529	Baolo	0,7	7	,3	9		3	9	3	6		4	8		,0
PBL_C17_3_2_3	Puen		18,	70				1,	0,	1,		7,			100
119	Baolo	0,6	6	,5				4	6	0		4			,0
DF_1_A_4_131	Thong Na		21,	67	0,			4,	0,	0,		2,	1,		100
_a	Nguak	0,8	8	,8	6			1	7	8		0	4		,0
DF_1_A_4_131	Thong Na	0,6	17,	74		0,	0,	2,	0,	0,		3,	0,		100

_b	Nguak		8	,4		3	2	1	1	6		0	9			,0
	Thong Na		22,	67	0,		0,	2,	0,	0,		5,	0,			100
DF_1_A_B3_90	Nguak	0,6	0	,3	5		3	3	4	6	0,2	3	6			,0
	Thong Na		24,	68			0,	3,	0,	0,		2,				100
DF_1_C_2	Nguak	0,8	9	,2			2	1	4	4		0				,0
	Thong Na		20,	66				3,	0,	0,		6,	1,			100
DF_3_37	Nguak	0,7	7	,9				0	1	8	0,4	3	1			,0
	Thong Na		20,	69			0,	2,	0,	0,		3,	0,		0,	99,
DF_1_B_113	Nguak	0,8	6	,7			4	7	5	7	0,1	5	3		7	3
Mean		0,7	22, 1	68 ,2	0, 3	0, 1	0, 2	2, 5	0, 4	0, 8	0,1	4, 2	0, 6	0, 0	0, 0	

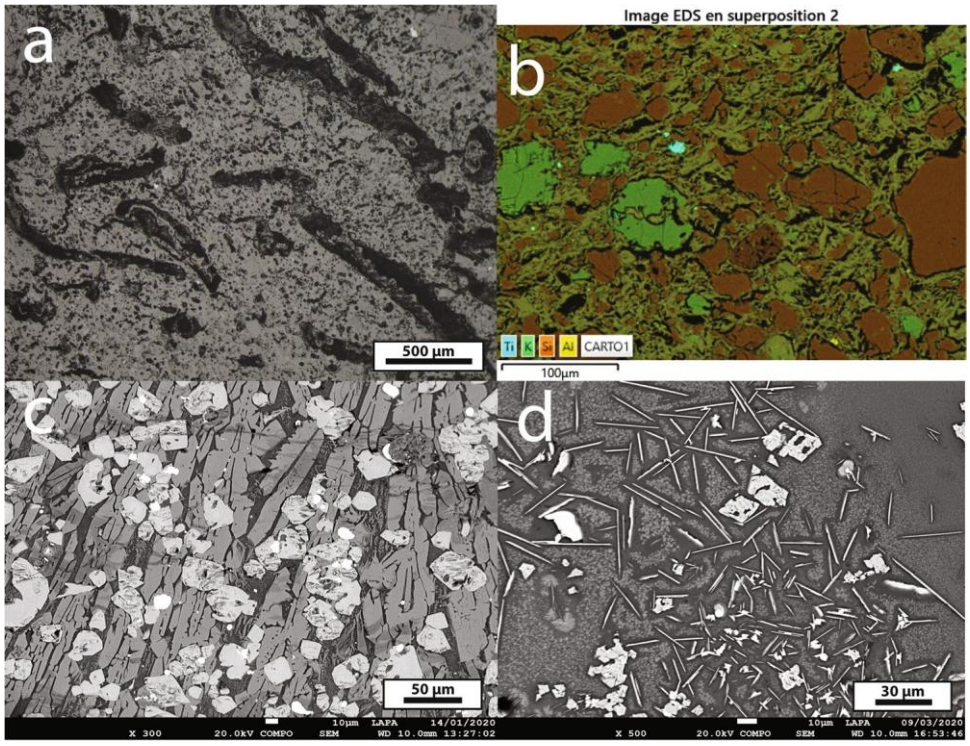

*Figure 8 : **a** OM image of the crucible paste of sample PBL/ A15/4/1/6709/b with rice chaff voids; **b** SEM–EDS X-ray map (Kα ROIs) of the crucible paste of sample PBL/B17/2/1/3303/f zone containing potassium feldspars, quartz grains and rutile identified by their composition and habits; **c** SEM-BSE image with an example of fayalitic lattices in the interior of the crucible PBL/C14/2/3/7217; **d** SEMBSE image with an example of a vitreous copper-rich slag for the sample DF/1-A/4/131/a with delafossite needles*

Four samples (SEALIP/LA/PBL/42, 48, 51 and 52) have a layer composed of copper sulphide (Table 6) and have been identified as matte on its average composition of Cu (71.5 wt%), S (21.5 wt%) and Fe (0.9 wt%) as well as its blue lamellar structure under OM.
The slag layer is identified for four samples (SEALIP/LA/ PBL/49, 50, 51 and BB14/3/3/7113). The main components of the slags are iron oxide (59 wt%), silica (28 wt%) and alumina (5.5 wt%) such as for the 'independent' slags from PBL and TNN. Other minor components are also present: CaO (2 wt%), CuO (2 wt%), MnO (1.5 wt%), K2O (0.7 wt%) and MgO (0.5 wt%). Concerning the microstructure, the main crystals are the same as the 'independent' slags: fayalite crystals, magnetite in a glassy matrix along with metallic copper and copper sulphide

inclusions. The microstructure and composition of the slags from the multi-layered artefacts and the 'independent' slags appear the same.

Discussion

Assessment of the chaîne opératoire

Nature of ore used and process

Compositional data from slag and crucible slags suggests VC production was limited to copper, with no traces of alloying components like tin or lead. Therefore, one of the questions this study addressed was the identification of the type(s) of ore(s) used for the copper production. This largely determines the complexity of the metallurgical process (Rostoker et al. 1989; Edmonds 1990): oxidic/ carbonate ores are associated with a one-step process vs sulfidic ores associated with a multi-step process. The Vilabouly Complex has extensive evidence of mining activity, in the form of abundant mining shafts. The ores used in the reduction process at the VC can therefore be assumed, as a first approximation, to be local. The vast majority (10 of 15) of ore samples are identified as malachite (Cu2CO3(OH)2), a copper carbonate associated with other minerals such as cuprite (CuO), quartz (SiO2), goethite (α-FeOOH). All these ores come from the upper, supergene, layer of the copper mineralization. Although they were discovered in archaeological contexts, especially at PBL, we cannot be sure whether these were minerals sorted and selected, or on the other hand, rejected by VC smelters.

Referring to the VC geological information summarized above, we note that malachite as well as other copper oxides/ carbonates (azurite, cuprite) are present in abundance in the weathered layers of mineralization accessible by former metallurgists within 40 m of the surface. Also identified is the abundant presence of a secondary copper sulphide, chalcocite (Cu2S), near and sometimes even mixed with oxide/carbonate deposits. Complex sulphide ores are also present, chalcopyrite (CuFeS2) and pyrite (FeS) as well as a low level of bornite (Cu5FeS4). The identification of copper sulphide inclusions in the smelting slag corpus implies three possibilities: inclusions of copper sulphides in a carbonate/ oxidized ore; the use of a multi-stage process with reduction of complex sulphide ores with matte production; or a hybrid process with a mixture of carbonate/oxidized and sulphide ores (Rostoker et al. 1989; Rostoker and Dvorak 1991). This ore mixture may be intentional or unintentional depending on the mineralization being mined and the knowledge of former metallurgists, as defined for the Khao Wong Prachan Valley in Thailand (Pryce et al. 2010).

Table 4 : Chemical composition of the slag adhering to the crucibles (SEM–EDS, wt%). < ld. = below detection limit

Sample	MgO	Al_2O_3	SiO_2	P_2O_5	SO_3	K_2O	CaO	TiO_2	MnO	FeO	CuO	ZnO	BaO
A15_3_1_6703	1,1	14,5	54,1			2,9	2,1	0,5	0,4	17,8	6,5		
A15_4_1_5709_b	0,9	13,8	53,7	0,4		2,6	0,6	0,6	0,2	17,9	9,5		
B14_1_1_7001_a	0,7	7,9	28,7	0,5	0,6	1,6	1,4	0,5	1,5	54,5	1,7	0,5	
B17_2_2_3314_a	1,0	10,7	41,7			2,3	1,1	0,4	0,3	18,9	23,5	0,2	
C14_2_3_7217	0,7	5,1	22,5			0,5	0,7	0,2	0,9	66,9	2,5		
C17_1_2_b	0,6	14,8	62,5	0,3		3,1	0,4	0,5		12,6	5,3		
D13_2_1_3706_b	0,7	7,4	24,8	0,8		0,4	0,4	0,2	0,7	63,5	0,8	0,3	
DD14_2_1_7123_a	1,0	12,9	45,7	0,6		2,5	2,3	0,0	2,8	19,3	1,7		11,2
E15_3225_a	0,8	5,7	38,4	0,7		0,8	0,6	0,2	0,7	49,1	2,7		
S9_1_1_5503	0,7	10,7	44,3			1,8	1,6	0,6	0,3	24,9	14,9	0,2	
C14_2_1_7209_a	0,5	4,2	37,7	0,3		0,6	0,4	0,2	0,6	52,8	2,5	0,2	

B17_2_1_3303_h	0,4	3,9	30,2	0,4		0,5	0,3	0,2	3,5	58,1	1,5	0,4	0,7
G15_3_4_7316_d	1,2	5,9	45,5		1,6	0,8	1,0	0,4	3,2	36,4	3,9		
G15_3_1_7309_7303_b	0,9	10,5	41,9	0,6		1,3	1,3	0,4	0,9	41,7	0,6		
E15_2_1_3211	0,5	8,6	36,6			0,7	0,4	0,3	1,0	47,6	4,4		
WEST_1_2_3	5,1	7,7	35,0			1,0	1,4	0,4	0,7	47,5	1,2		
D13_2_1_3706_a	0,5	8,6	32,3		0,2	1,3	0,4	0,5	0,3	55,2	0,8		
G15_3_3_3311_c	1,2	10,7	38,0			1,3	1,6		1,6	45,1	0,7		
C16_3_1_3529	0,7	6,8	36,8		0,4	0,9	0,8		1,8	50,1	1,7		
C17_2_3_3119	1,4	12,6	62,1			2,3	6,6	0,7		6,4	7,9		
DF_1_A_4_131_a	1,2	13,3	50,5	1,1		3,9	3,7	0,6	1,3	7,9	15,1	1,1	0,2
DF_1_A_4_131_b	0,8	9,6	46,0	0,6		2,8	1,6	0,4	1,8	28,4	6,0	1,8	0,2
DF_1_A_B3_90	0,6	12,5	46,6			2,3	0,8	0,4	1,1	26,5	8,6	0,5	0,0
DF_1_C_2	0,6	12,3	42,4			2,3	1,6	0,2	5,4	13,7	19,3	1,5	0,7
DF_3_37	0,6	12,6	45,1			2,5	0,3	0,5	7,6	21,3	6,9	1,9	0,7
DF_1_B_113	0,5	9,5	36,9			1,6	0,6	0,3	0,1	49,2	0,8	0,1	0,4
Mean	1,0	9,7	41,5	0,2	0,1	1,7	1,3	0,4	1,5	35,9	5,8	0,4	0,5

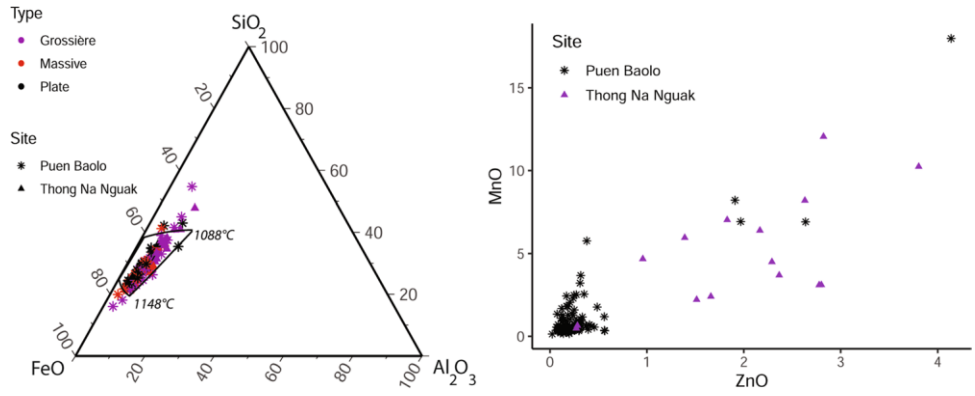

Figure 9 : Left: Ternary diagram showing the major component of the slags (SiO2, Al2O3 and FeO) by type of slags for PBL and TNN with the fayalitic field after Rehren et al. (2007). Right: Comparison of the composition in MnO and ZnO for PBL and TNN (ICP-MS/ ICP-OES, wt%)

The presence of sulfidic phases in slag does not prove the use of a complex process with matte production (Hauptmann 2007; Rehren et al. 2012), but layers of macroscopic matte are also present at the VC in the multi-layered artefacts. The identification of macroscopic matte here reinforces our questioning of the type(s) of ore(s). These artefacts with a macroscopic layer of matte were interpreted as coming directly from the reduction step. These questions led us to set up experimental reconstruction of reductions with different mixtures of ores (malachite, chalcocite and chalcopyrite). The detailed results of these experiments are the subject of another publication (Cadet et al. 2021) but in summary the replicated ore mixtures, including malachite/chalcocite, resulted in a by-product comparable to the archaeological example, with a layer of metallic copper covered by a layer of matte. Data suggests that the production process of Vilabouly could be a co-smelting. This co-smelting would be preferentially composed of malachite and chalcocite, being the two main ores available in near-surface mineralizations, sometimes including chalcopyrite, and possibly pyrite and bornite but their contribution is difficult to estimate. This process appears dependent on the mineralization being exploited. The presence and perhaps even

the nature of sulphide ores in the charge appear variable. Presumably, the purpose of the process was not to produce matte, but rather to produce metallic copper directly by co-smelting. Indeed, the amount of copper produced seems variable when looking at the multi-layered artefacts. Their composition is then linked to the charge and the condition during the process, which appears variable regarding the different multi-layered artefacts obtained. Furthermore, the matte did not seem to have been reprocess, which makes us ask the question of the knowledge of ancient metallurgists concerning the reuse of matte. It is also important to note, however, that most of these matte-rich artefacts are from a mortuary context. Thus, it is possible that they represent work that the deceased was engaged in at the time of death.

Slag formation

The two main slag compounds, silica and iron oxide, allow the formation of a low-melting point (1100–1150 °C) fayalitic slag and must be accounted for by the charge (ore, gangue, flux, fuel) and/or degrading ceramics (crucibles, tuyères, furnaces). The slag elemental data were represented in a FeO-SiO2-Al2O3 phase diagram, as these three compounds account for about 90% of the total. In addition, VC slag is homogeneous with few unreacted inclusions, indicating it fully liquefied allowing a representation on a ternary diagram. PBL and TNN slags fall mainly in the field of fayalite (Fig. 9), with some notable exceptions. PBL slags appear closer to the optimum 2 of 1148 °C defined for iron metallurgy by Rehren et al. (2007) but arguably applicable to that of copper, whereas TNN slags approach optimum 1 at around 1100 °C. The form and homogeneity of the flat slags suggest temperatures in excess of 1100–1200 °C. Indeed, using Kresten's (1986) forsterite-fayalite binary diagram suggests about 1210–1220 °C for PBL and TNN. These higher temperatures could allow the formation of homogeneous low viscosity flat slags (Burger 2008). The smelting charge therefore had a balance suitable for the production of slags of the fayalitic type, which means a molar ratio of Fe/Si close to 2.

Comparing the composition of the oxides from the slags, crucibles and ores (Fig. 14), the main differences can be seen in the iron oxide content, which is much higher for the slags. Because copper is taking out of the system, its content decreases in the slags and may also explain in part the enrichment of iron in the slags. Following this logic, silica should be higher because it is more present in ores than iron. Iron oxide content cannot come from a contribution from the crucible clay as the iron oxide content is even lower (≈4wt%). This could mean that an iron oxide-rich mineral could have been added as a flux to the smelting charge to obtain this type of fayalitic slag. This would indicate an adaptation and knowledge of the ancient metallurgists to make the process more efficient. Iron ores are abundant at the Vilabouly complex due to the presence of a gossan on the deposits, would thus have been easy to access. The results for the ores have shown that haematite and goethite are part of the assemblage from VC and could constitute the iron minerals added. However, a contribution from the crucible paste to the slag composition can be shown by Al2O3 content which is higher in the paste and slags than in the ore. MnO content is also higher in the slags than for ore and clay, confirming that unknown minerals with higher MnO content should be part of the mineral assemblage to consider, in particular for TNN. These results may show that our assemblage must include unknowns, such as the sulfidic ores, the manganese-rich mineral probably for TNN and potential iron oxide mineral that may influence the interpretations for the smelting charge.

Table 5 : Bulk composition of the independent slags (ICP-MS/ICP-OES, wt%)

Sample	Site	Type	SiO_2	Al_2O_3	FeO	MnO	MgO	CaO	Na_2O	K_2O	TiO_2	P_2O_5	CuO	ZnO	SO_3	BaO
G15_1_3_7304_a	PBL	Flat	33,5	4,3	58,5	0,2	0,7	0,2	0,0	0,5	0,2	0,3	1,0	0,1	0,5	0,0
G15_1_3_7304_b	PBL	Coarse	49,1	5,6	35,1	1,8	1,1	0,9	0,0	0,6	0,3	0,6	4,6	0,2	0,1	0,1
G15_1_3_7304_c	PBL	Massive	21,8	4,9	64,8	2,3	0,8	1,5	0,0	0,4	0,4	0,5	1,6	0,2	0,6	0,1
G15_2_3_7308_a	PBL	Flat	26,9	5,4	63,2	0,5	0,8	0,2	0,0	0,6	0,3	0,5	1,3	0,2	0,2	0,0
G15_2_2_7305_b	PBL	Flat	39,8	4,2	50,4	0,4	0,5	0,9	0,0	0,7	0,4	0,3	0,9	0,6	0,8	0,1
G15_2_2_7305_c	PBL	Massive	20,7	3,5	71,0	0,3	0,5	0,5	0,0	0,2	0,2	0,3	1,1	0,1	1,7	0,0
G15_2_2_7305_f	PBL	Flat	40,2	8,7	44,4	0,5	0,9	0,3	0,0	1,7	0,4	0,4	2,0	0,2	0,3	0,0
G15_2_2_7305_g	PBL	Flat	22,0	4,4	69,0	0,3	0,4	0,2	0,0	0,2	0,3	0,3	1,3	0,1	1,3	0,0
G15_2_2_7305_h	PBL	Coarse	24,8	8,6	61,0	0,6	0,9	0,5	0,0	0,7	0,4	0,4	1,2	0,4	0,6	0,1
G15_2_3_7308_b	PBL	Massive	22,8	5,1	64,4	0,5	0,6	0,3	0,0	1,0	0,3	0,5	3,7	0,2	0,6	0,0
G15_3_1_7309_a	PBL	Flat	21,4	3,6	71,0	0,4	0,5	0,4	0,0	0,4	0,2	0,4	1,0	0,1	0,5	0,0
G15_3_2_7310_a	PBL	Flat	24,4	3,3	68,4	0,5	0,4	0,4	0,0	0,5	0,2	0,3	1,1	0,1	0,5	0,0
G15_3_2_7310_b	PBL	Massive	32,7	7,0	51,8	1,8	1,3	1,0	0,0	0,7	0,3	0,7	1,4	0,5	0,7	0,1
G15_3_2_7310_c	PBL	Coarse	25,8	5,7	60,0	0,6	0,5	0,4	0,0	1,0	0,3	0,4	4,6	0,3	0,4	0,0
G15_3_2_7310_d	PBL	Coarse	28,4	5,3	60,8	0,5	0,6	0,5	0,0	0,8	0,4	0,4	1,4	0,3	0,4	0,1
G15_3_3_7311_a	PBL	Flat	21,8	3,5	69,8	0,4	0,4	0,5	0,0	0,5	0,2	0,4	1,3	0,1	0,9	0,0
G15_3_3_7311_e	PBL	Massive	35,1	3,6	46,4	3,2	4,1	4,2	0,0	0,4	0,1	0,6	1,5	0,3	0,1	0,3
G15_3_4_7316_7306	PBL	Flat	27,8	4,7	59,8	0,4	0,5	0,6	0,0	0,9	0,3	0,3	3,8	0,2	0,6	0,0
G15_3_4_7316_a	PBL	Coarse	26,6	4,3	64,8	0,5	0,5	0,3		0,7	0,3	0,3	1,0	0,2	0,5	0,0
G15_3_4_7316_b	PBL	Flat	21,2	4,3	68,9	0,3	0,5	0,3	0,0	0,8	0,2	0,3	1,4	0,1	1,6	0,0
G15_3_4_7316_c	PBL	Massive	27,2	5,1	62,6	0,4	0,5	0,4	0,0	0,7	0,3	0,4	1,5	0,1	0,6	0,0
E15_1_2_3204_a	PBL	Massive	26,6	5,4	59,3	0,5	0,4	0,4	0,0	0,8	0,4	0,3	3,9	0,3	1,0	0,5
E15_1_2_3204_b	PBL	Flat	21,8	4,5	68,6	0,9	0,5	0,3	0,0	0,6	0,3	0,4	1,0	0,3	0,9	0,0
E15_1_2_3204_c	PBL	Coarse	37,7	7,0	46,0	1,0	0,9	0,7	0,0	0,8	0,3	0,5	4,8	0,3	0,1	0,1
E15_2_2_3218_b	PBL	Coarse	35,3	4,8	50,4	0,2	0,5	0,2	0,0	0,6	0,2	0,3	2,5	0,1	4,9	0,0
E15_2_2_3218_c	PBL	Coarse	25,0	5,6	62,2	0,3	0,5	0,5	0,0	0,9	0,3	0,6	3,3	0,3	0,3	0,0
E15_2_2_3218_d	PBL	Coarse	26,1	4,7	64,8	0,5	0,5	0,3	0,0	0,6	0,3	0,3	0,9	0,2	0,5	0,1
E15_2_2_3218_e	PBL	Flat	25,	4,1	65,	0,5	0,4	0,4	0,0	0,7	0,3	0,4	0,8	0,2	2,0	0,0

			0		2												
			28,		61,												
E15_2_3_3230_c	PBL	Flat	0	5,6	4	0,4	0,6	0,4	0,1	0,9	0,3	0,3	1,0	0,1	0,7	0,1	
			29,		59,												
E15_2_3_3247_b	PBL	Coarse	2	5,9	8	0,3	0,7	0,4	0,0	0,7	0,3	0,3	1,0	0,2	1,2	0,0	
			34,		49,												
E15_3_1_3277_b	PBL	Coarse	0	7,1	7	1,8	0,7	1,2	0,1	1,1	0,4	0,5	2,8	0,2	0,3	0,2	
			25,		61,												
E15_3_1_3277_c	PBL	Coarse	2	4,6	9	0,9	0,5	0,5	0,0	0,8	0,3	0,4	4,2	0,3	0,3	0,1	
		Massiv	25,		63,												
C17_1_1_3117_a	PBL	e	8	4,8	3	0,4	0,6	0,4	0,0	1,1	0,3	0,2	1,9	0,3	0,9	0,0	
		Massiv	32,		55,												
C17_1_1_3117_b	PBL	e	2	6,1	7	0,6	0,4	0,3	0,1	1,1	0,3	0,2	2,4	0,1	0,5	0,1	
			25,		62,												
C17_1_1_3117_c	PBL	Coarse	9	3,9	1	1,0	0,5	0,1	0,0	0,3	0,2	0,4	2,6	0,2	2,6	0,1	
			28,		59,												
C17_1_1_3117_d	PBL	Coarse	2	4,1	9	2,5	0,6	0,3	0,0	0,4	0,4	0,6	1,9	0,3	0,4	0,3	
		Massiv	25,		64,												
C17_1_2	PBL	e	9	4,0	9	0,9	0,6	0,6	0,0	0,5	0,4	0,5	0,8	0,2	0,6	0,0	
			15,		78,												
C17_1_2_a	PBL	Coarse	6	2,7	9	0,1	0,2	0,6	0,0	0,3	0,2	0,7	0,4	0,0	0,4	0,0	
			27,		64,												
C17_1_2_c	PBL	Flat	4	4,2	1	0,2	0,5	0,1	0,0	0,4	0,2	0,3	0,5	0,1	2,0	0,0	
			29,		60,												
C17_1_2_d	PBL	Flat	0	5,0	0	0,4	0,5	0,8	0,0	0,9	0,3	0,3	1,7	0,2	0,7	0,1	
			30,		57,												
C17_1_2_f	PBL	Coarse	8	5,9	9	0,5	0,6	0,2	0,0	0,9	0,3	0,3	1,9	0,2	0,4	0,0	
		Massiv	20,		69,												
C17_2_1_3107_b	PBL	e	3	4,9	6	0,4	0,4	0,1	0,0	0,6	0,3	0,3	2,0	0,3	1,0	0,0	
			41,		43,												
C17_2_1_3107_c	PBL	Coarse	7	7,5	5	1,1	0,6	0,2	0,0	1,1	0,4	0,5	2,9	0,1	0,2	0,3	
			29,		51,												
C17_2_1_3107_e	PBL	Coarse	2	5,4	7	2,1	0,5	2,2	0,0	1,0	0,3	0,3	6,6	0,2	0,1	0,3	
			26,		62,												
B14_1_1_7001_b	PBL	Coarse	0	5,8	5	0,5	0,5	0,5	0,0	0,9	0,3	0,3	2,1	0,2	0,4	0,0	
			26,		62,												
B14_1_1_7001_c	PBL	Flat	4	4,8	9	0,5	0,5	0,4	0,0	0,8	0,4	0,4	1,3	0,2	1,4	0,1	
			20,		68,												
B14_1_2_7002_b	PBL	Flat	5	4,5	0	0,5	0,4	0,2	0,0	0,6	0,3	0,3	2,1	0,3	2,2	0,0	
		Massiv	21,		66,												
B14_1_2_7002_c	PBL	e	6	3,4	6	1,0	0,3	0,2	0,0	0,2	0,2	0,5	2,3	0,1	3,3	0,1	
			28,		63,												
B14_2_1_7003	PBL	Flat	2	4,0	0	0,5	0,5	0,3	0,0	0,6	0,3	0,3	1,4	0,2	0,4	0,1	
			27,		62,												
CC14_1_1_a	PBL	Coarse	8	5,0	6	1,2	0,6	0,3	0,0	0,4	0,2	0,4	1,0	0,3	0,3	0,0	
			28,		60,												
CC14_1_1_b	PBL	Flat	2	5,3	3	0,5	0,6	0,3	0,0	0,9	0,4	0,4	1,8	0,2	1,0	0,0	
		Massiv	30,		55,												
CC14_1_1_c	PBL	e	7	6,0	5	0,7	0,7	0,5	0,0	1,2	0,4	0,3	3,4	0,2	0,3	0,1	
			26,		64,												
CC14_3_7116_a	PBL	Flat	5	3,6	9	0,4	0,3	0,3	0,0	0,4	0,2	0,4	0,6	0,2	2,2	0,0	
			28,		57,												
CC14_3_7116_b	PBL	Coarse	9	5,1	4	0,4	0,4	0,4	0,0	0,9	0,3	0,3	5,0	0,3	0,5	0,0	
		Massiv	25,		59,												
CC14_3_7116_c	PBL	e	0	7,1	9	0,5	0,8	0,4	0,0	1,2	0,4	0,4	3,2	0,2	0,9	0,1	
			17,		74,												
CC14_3_7116_d	PBL	Coarse	4	4,3	4	0,3	0,4	0,1	0,0	0,3	0,3	0,4	0,9	0,6	0,6	0,0	

CC14_3_7116_e	PBL	Flat	27,6	4,5	63,4	0,5	0,6	0,2	0,0	0,6	0,2	0,6	0,5	0,2	1,0	0,0
CC14_3_7116_f	PBL	Coarse	26,5	5,3	58,3	0,5	0,5	0,6	0,0	0,8	0,3	0,4	5,9	0,2	0,5	0,1
CC14_3_7116_g	PBL	Coarse	26,2	5,1	62,3	1,0	0,6	0,3	0,0	1,0	0,3	0,5	2,1	0,3	0,4	0,1
DD14_1_1_7108	PBL	Coarse	24,6	4,7	62,7	0,6	0,5	0,4	0,0	1,0	0,3	0,4	3,5	0,4	0,8	0,0
A15_2_2_6703	PBL	Flat	26,2	4,8	64,4	0,4	0,5	0,2	0,0	0,6	0,2	0,3	1,8	0,1	0,4	0,0
A15_3_1_6705_a	PBL	Massive	20,7	3,0	71,9	0,4	0,2	0,2	0,0	0,2	0,2	0,2	1,3	0,1	1,5	0,0
A15_3_1_6705_b	PBL	Coarse	24,0	3,8	68,0	0,3	0,4	0,2	0,0	0,5	0,3	0,8	1,3	0,2	0,4	0,0
A15_3_1_6705_c	PBL	Flat	24,7	4,3	65,5	0,5	0,5	0,3	0,0	0,7	0,3	0,4	1,7	0,2	0,8	0,0
A15_4_1_6712	PBL	Flat	29,2	4,4	62,6	0,3	0,6	0,2	0,0	0,6	0,2	0,2	0,5	0,1	0,9	0,0
AA15_2_2_6803_b	PBL	Flat	29,4	5,4	56,2	2,6	0,6	1,8	0,0	1,0	0,3	0,3	1,0	0,4	0,8	0,2
AA15_2_3_6811_a	PBL	Flat	29,2	6,3	59,8	0,4	0,7	0,3	0,0	0,8	0,3	0,3	0,7	0,2	0,9	0,0
AA15_2_3_6811_b	PBL	Massive	29,6	5,4	60,2	0,4	0,5	0,4	0,0	0,9	0,3	0,3	1,1	0,1	0,7	0,0
AA15_2_3_6811_c	PBL	Coarse	25,8	4,6	61,8	0,6	0,5	0,6	0,0	0,9	0,3	0,4	3,7	0,3	0,4	0,1
AA15_3_1_6808_b	PBL	Coarse	20,3	5,4	62,9	2,5	1,3	0,9	0,0	0,4	0,3	0,4	2,2	0,2	1,4	1,7
AA15_3_1_6808_d	PBL	Massive	18,6	2,1	72,9	1,0	0,3	0,6	0,0	0,2	0,1	0,2	1,7	0,1	2,1	0,0
AA15_3_1_6808_e	PBL	Flat	20,9	3,4	70,8	0,7	0,3	0,3	0,0	0,4	0,2	0,3	1,6	0,3	0,7	0,0
AA15_4_1_6818	PBL	Flat	26,4	4,9	63,1	0,7	0,5	0,2	0,0	0,7	0,2	0,5	1,0	0,4	1,2	0,0
AA15_4_2_6822_a	PBL	Coarse	34,7	7,3	53,1	0,4	0,7	0,3	0,0	1,1	0,3	0,4	1,0	0,2	0,3	0,1
AA15_4_3_6826	PBL	Flat	33,5	4,2	58,1	0,3	0,8	0,3	0,0	0,4	0,2	0,3	1,4	0,2	0,4	0,0
C14_1_3_7204_a	PBL	Flat	23,8	5,3	64,4	1,0	0,6	0,7	0,1	0,9	0,3	0,1	1,9	0,3	0,6	0,1
C14_1_3_7204_b	PBL	Massive	21,8	5,2	62,6	0,2	0,5	0,2	0,1	0,8	0,3	0,0	7,0	0,2	1,1	0,1
C14_1_4_7205_a	PBL	Coarse	20,1	5,8	55,7	5,8	0,4	0,1	0,0	0,8	0,3	2,0	1,6	0,4	1,0	6,1
C14_1_4_7205_b	PBL	Massive	22,1	3,1	68,5	0,5	0,4	0,3	0,0	0,4	0,2	0,5	2,4	0,2	1,4	0,0
C14_1_4_7205_c	PBL	Flat	31,0	10,5	46,1	1,6	2,2	2,4	0,0	1,0	0,5	0,4	2,3	0,3	0,6	1,0
C14_1_4_7205_d	PBL	Coarse	24,4	4,6	64,6	0,4	0,5	0,3	0,0	0,8	0,3	0,6	2,5	0,4	0,5	0,0
C14_2_1_7209_b	PBL	Coarse	29,0	5,5	57,4	0,4	0,5	0,4	0,0	1,0	0,3	0,3	4,6	0,1	0,4	0,0
C14_2_3_7219_a	PBL	Massive	23,8	3,5	67,2	0,5	0,2	0,2	0,0	0,3	0,2	0,7	1,9	0,1	1,5	0,0
C14_2_3_7219_b	PBL	Coarse	26,6	4,9	60,8	0,5	0,4	0,4	0,0	0,8	0,3	0,8	3,7	0,2	0,5	0,1
C14_2_3_7219_c	PBL	Flat	25,	4,3	64,	0,6	0,5	0,6	0,0	0,7	0,3	0,7	1,3	0,2	0,5	0,1

			7		7											
			26,		60,											
B17_1_1_3301_a	PBL	Coarse	5	5,2	0	1,3	0,6	1,2	0,0	0,7	0,4	0,8	2,2	0,2	0,7	0,1
		Massiv	29,		57,											
B17_1_1_3301_b	PBL	e	8	5,5	5	1,3	0,6	0,9	0,0	0,6	0,4	0,7	0,7	0,1	1,7	0,1
			23,		69,											
B17_1_1_3301_c	PBL	Flat	3	3,5	0	0,4	0,4	0,2	0,0	0,4	0,2	0,4	0,8	0,3	1,0	0,0
			20,		65,											
B17_2_1_3303_a	PBL	Coarse	2	3,9	5	2,4	1,0	2,4	0,0	0,4	0,8	1,0	1,2	0,2	0,7	0,3
		Massiv	25,		66,											
B17_2_1_3303_b	PBL	e	1	3,6	0	0,6	0,6	0,6	0,0	0,5	0,2	0,4	1,0	0,5	0,9	0,0
			29,		60,											
B17_2_1_3303_c	PBL	Coarse	3	5,0	6	0,6	0,4	0,2	0,0	0,8	0,2	0,5	1,3	0,2	0,7	0,2
		Massiv	21,		71,											
B17_2_1_3303_d	PBL	e	3	3,5	5	0,5	0,4	0,2	0,0	0,3	0,2	0,5	0,6	0,2	0,9	0,0
			28,		60,											
B17_2_1_3303_i	PBL	Flat	8	4,9	8	0,4	0,6	0,8	0,0	0,8	0,3	0,4	1,3	0,2	0,6	0,1
		Massiv	27,		58,											
B17_2_1_3303_j	PBL	e	3	5,4	9	0,9	0,5	2,0	0,0	0,8	0,4	0,5	2,3	0,1	0,8	0,1
			19,		67,											
B17_2_2_3311_a	PBL	Coarse	5	4,6	1	1,7	0,8	1,6	0,0	0,4	0,9	0,5	0,9	0,1	1,3	0,6
		Massiv	23,		66,											
B17_2_2_3311_b	PBL	e	1	4,3	0	0,3	0,3	0,5	0,0	0,8	0,2	0,2	2,9	0,2	0,8	0,2
			29,		53,											
B17_2_2_3314_b	PBL	Coarse	8	7,5	0	1,3	0,9	1,2	0,0	1,3	0,6	0,6	2,5	0,1	0,6	0,5
			22,		71,											
B17_3_1_3312_b	PBL	Flat	6	3,2	3	0,5	0,4	0,1	0,0	0,1	0,2	0,4	0,4	0,1	0,6	0,0
			30,		57,											
B17_3_1_3312_c	PBL	Coarse	3	6,0	3	1,4	0,7	0,8	0,0	0,7	0,4	0,5	1,4	0,2	0,2	0,1
		Massiv	26,		61,											
B17_3_1_3312_d	PBL	e	8	5,5	4	0,7	0,7	1,5	0,0	0,7	0,3	0,3	1,4	0,1	0,4	0,1
			25,		66,											
C16_1_1	PBL	Flat	1	4,6	2	0,3	0,4	0,3	0,0	0,6	0,2	0,0	1,4	0,2	0,8	0,0
C16_GENSPIT_350			22,		68,											
1_a	PBL	Flat	4	4,3	5	0,4	0,5	0,3	0,0	0,7	0,2	0,0	1,8	0,2	0,7	0,0
C16_GENSPIT_350		Massiv	24,		59,											
1_b	PBL	e	9	4,5	5	0,3	0,4	0,2	0,0	0,6	0,2	0,1	8,2	0,2	0,8	0,0
		Massiv	26,		59,											
C16_3503_a	PBL	e	8	6,7	1	0,6	0,5	0,8	0,0	0,7	0,4	0,0	3,6	0,1	0,7	0,1
			25,		64,											
C16_3503_b	PBL	Flat	7	4,3	4	0,6	0,5	0,7	0,0	0,8	0,2	0,0	1,5	0,2	1,0	0,0
			26,		60,											
C16_3503_c	PBL	Coarse	1	4,8	2	3,7	0,6	0,4	0,0	0,5	0,2	0,0	2,5	0,3	0,3	0,3
			23,		70,											
C16_3_1_3524	PBL	Flat	6	2,9	2	0,4	0,3	0,1	0,0	0,3	0,2	0,0	0,5	0,3	1,3	0,0
			21,		62,											
S9_1_1_5503_a	PBL	Coarse	6	4,3	3	6,9	0,5	0,3	0,0	0,3	0,2	0,4	0,6	2,0	0,4	0,2
		Massiv	21,		60,											
S9_1_1_5503_b	PBL	e	7	4,3	8	6,9	0,3	0,2	0,0	0,4	0,2	0,3	0,9	2,6	0,9	0,3
			27,		61,											
S9_2_2_5505_a	PBL	Flat	3	5,9	5	0,6	0,5	0,3	0,0	0,6	0,2	0,3	2,2	0,3	0,2	0,0
			24,		55,											
S9_2_2_5505_b	PBL	Coarse	6	5,2	7	8,2	0,7	0,4	0,0	0,6	0,3	0,3	0,9	1,9	0,8	0,5
			24,		45,											
S9_2_2_5508	PBL	Coarse	2	4,2	9	18,0	0,4	0,2	0,0	0,4	0,2	0,4	0,9	4,1	0,3	0,6
			29,		52,											
WEST1_1_2_b	PBL	Coarse	7	5,1	6	0,2	6,2	1,3	0,0	0,6	0,1	0,4	3,0	0,2	0,5	0,1

WEST1_1_2_c	PBL	Coarse	26,1	5,7	60,2	0,7	1,0	0,2	0,0	0,6	0,2	0,3	4,0	0,3	0,6	0,1
D13_3729_3704	PBL	Massive	20,3	3,0	70,4	0,3	0,2	0,4	0,0	0,5	0,2	0,2	3,4	0,2	0,9	0,0
PBL_1_4_269_97	PBL	Flat	28,0	3,8	61,4	0,4	0,5	0,2	0,0	0,7	0,2	1,0	1,7	0,1	2,0	0,0
PBL_2_8_359_349	PBL	Massive	32,1	5,6	55,5	1,3	0,7	0,5	0,0	0,6	0,2	0,4	2,3	0,2	0,5	0,1
PBL_2_3_361_302	PBL	Flat	31,7	4,8	57,8	0,5	0,3	0,5	0,0	0,9	0,2	0,2	0,7	0,1	2,1	0,0
PBL_2_10_333_365	PBL	Massive	29,3	4,4	61,6	0,3	0,2	0,4	0,0	0,6	0,2	0,2	1,8	0,1	0,8	0,0
PBL_2_14_313_200	PBL	Massive	27,5	5,7	59,4	1,2	0,8	0,5	0,0	0,4	0,2	0,5	2,6	0,6	0,7	0,1
PBL_2_6_321_310	PBL	Flat	23,9	5,1	65,9	0,8	0,6	0,4	0,0	0,6	0,4	0,3	0,7	0,3	1,0	0,0
PBL_1_6_292_167	PBL	Flat	27,9	5,2	60,7	0,6	0,8	0,7	0,0	0,9	0,4	0,4	0,8	0,4	1,0	0,1
DF_1-A_138_a	TN N	Coarse	37,1	8,2	32,3	6,4	0,7	0,6	0,1	1,7	0,4	0,1	9,8	2,2	0,1	0,4
DF_1-A_138_b	TN N	Coarse	34,9	8,4	42,0	6,0	0,6	0,7	0,0	1,6	0,4	1,5	2,2	1,4	0,1	0,5
DF_1-A_2_40	TN N	Coarse	26,9	6,7	54,4	4,5	0,5	0,4	0,0	1,1	0,3	0,9	0,9	2,3	0,8	0,2
DF_1-A_4_133	TN N	Flat	28,3	4,5	45,7	12,1	0,4	0,6	0,0	0,9	0,3	0,8	1,6	2,8	0,3	1,6
DF_1-A_4_165_a	TN N	Coarse	34,2	5,6	51,9	0,5	2,7	0,5	0,0	0,8	0,2	0,7	1,9	0,3	0,1	0,6
DF_1-A_4_165_b	TN N	Coarse	33,1	6,3	51,2	0,6	2,2	0,7	0,0	0,9	0,2	0,6	3,3	0,3	0,2	0,3
DF_1-B_2_42	TN N	Coarse	32,3	6,2	46,1	7,0	0,5	0,5	0,0	1,1	0,3	0,7	2,8	1,8	0,1	0,7
DF_1-B_3_93_a	TN N	Flat	28,2	6,5	54,3	3,1	0,7	0,4	0,0	0,8	0,4	1,2	1,2	2,8	0,3	0,1
DF_1-B_3_93_b	TN N	Coarse	29,9	6,0	53,7	3,7	0,4	0,3	0,0	1,0	0,3	0,8	1,0	2,4	0,4	0,2
DF_1-C_3_8_c	TN N	Coarse	32,7	6,6	40,8	8,2	0,6	0,6	0,0	1,2	0,3	0,9	4,3	2,6	0,4	0,8
DF_1-D_3_99	TN N	Coarse	28,8	7,1	55,7	2,2	0,5	0,4	0,0	1,2	0,3	0,9	0,8	1,5	0,4	0,2
DF_1-E_2_39	TN N	Flat	23,1	3,4	64,1	4,7	0,4	0,3	0,0	0,3	1,5	0,5	0,4	1,0	0,2	0,1
DF_1-2_2_43	TN N	Massive	23,3	6,4	50,6	10,2	0,5	0,4	0,0	0,8	0,3	0,6	1,8	3,8	0,7	0,5
DF_1A-B_3_96_526	TN N	Coarse	31,4	6,8	49,7	3,1	0,6	0,5	0,0	1,2	0,4	1,1	2,1	2,8	0,2	0,2
DF_1-C_1_8_533	TN N	Coarse	28,1	7,3	45,7	2,4	0,5	0,3	0,0	1,2	0,4	0,9	10,5	1,7	0,7	0,2

With all these characteristics, the majority of the Vilabouly slag corresponds to the *plattenschlackle* described by Bachmann (1982) and identified in other contexts, mainly Alpine (Herdits 2003; Metten 2003; Burger 2008; Bourgarit et al. 2010; Addis et al. 2016), but also in Asia, in Tonglüshan, China, Hubei Province (Larreina-García 2017) and the Himalayas in Pokhri (Gupta. A, *person. Comm.*). This type of slag generally indicates a great mastery of the conditions leading to an optimal separation of metallic copper from its impurities (slag)

(Burger 2008; Bourgarit et al. 2010). The near absence of partially/unreacted inclusions reinforces this observation. On the other hand, the way in which this type of slag is formed is still debated. It is proposed that flat slags solidified rapidly on a molten liquid (copper or matte). They could therefore be obtained following rapid casting and cooling in contact with air. This is evidenced in particular by the presence of a magnetite band and acicular crystals, parallel to a surface, for most VC slags, which are usually associated with slag from casting processes (Hauptmann et al. 2003; Georgakopoulou et al. 2011). As the flat slags should solidify on another molten liquid, we hypothesize they could be associated to the multi-layered artefacts, poured together following the smelting step. Flat slag fragments do not exceed 5 cm in length but are fragmentary which makes it difficult to interpret their full state. The flat slags could then be removed from the matte/copper in order to recover metallic copper (and matte) only. How well the VC smelters understood matte remains unclear.

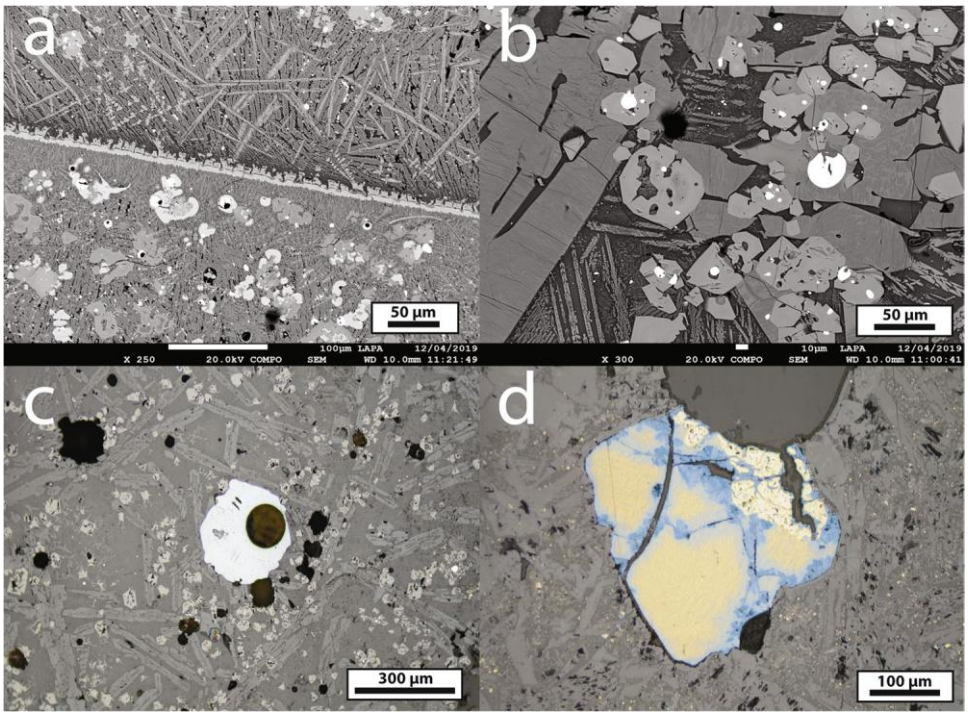

*Figure 10 : OM (bottom) and SEMBSE (top) images of the slags: **a** SEM BSE image of the slag PBL/B14/1/2/7002/b showing magnetite band, acicular and polyhedral magnetite as well as fayalite crystals and metallic inclusions; **b** SEM BSE image of PBL/C16/3503/a showing polyhedral magnetite, fayalite crystals and metallic inclusions; **c** OM image of the slag DF/1/A/4/165/b showing inclusions of secondary sulphide mineral chalcocite, fayalite crystals and magnetite; **d** OM image of the slag PBL/B17/1/1/3301/b showing a partially reacted ore grain composed of chalcopyrite and covellite*

Crucibles as reaction vessels

The VC crucibles possess the characteristics of early metallurgical crucibles identified elsewhere (Rehren 2003; Bayley and Rehren 2007; Rademakers 2015): traces of internal heating visible by a colour gradient from inside to outside, an internal slag layer, an open and shallow form with a convex bottom, showing they were not sitting on a flat surface but probably on charcoal/wood. Such vessels are usually small, here with a maximum diameter of 150 mm. Therefore, it offers a more limited usable volume, but allows for precise control of temperature and atmosphere without a furnace. Regarding the crucible paste, we identify a non-calcareous alumina-rich clay, with the strong presence of quartz inclusions and an

organic temper for most of the fragments: rice chaff. Rice chaff is frequently encountered in domestic and technical ceramics of Southeast Asia (Vernon 1996; Vincent 2003; Pryce et al. 2010; Tomber et al. 2011; Cawte 2012; Carratoni et al. 2018; Vernon et al. 2018). In this sense, the addition of rice chaff does not appear specific to metallurgy but belonging to a broader ceramic tradition.

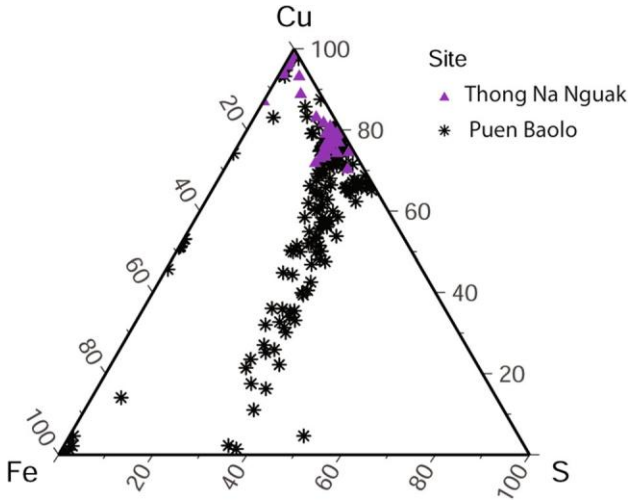

Figure 11 : Ternary diagram with the copper, iron and sulphur content (SEM–EDS, wt%) of the metallic inclusions in the slags from PBL (N=290) and TNN (N=73)

The slags identified in the crucibles could result from a pollution by the crucible paste, in particular for the vitreous one (Fig. 12). Two types of crucible slag can be distinguished in the VC corpus. Fayalitic slag with the same characteristics as the 'independent' slag, and the glass-dominated slag with a higher copper content indicating more oxidizing conditions. The observed difference between these slags could mean two different uses or/and a great variability of charges/conditions associated with the crucible. Variations in crucible slag composition can be induced by four main factors: oxygen supply, temperature, cooling rate and then by charge variations (Rademakers 2015; Rademakers and Rehren 2016). The results show similar Al2O3/SiO2 ratios, suggesting the slags belong to the same step of the process. The vitreous slag, rich in copper, involved more oxidizing conditions which could also come from the location of slag in the crucible, with the lips having more oxidizing conditions. The fragmentary state of most crucibles did not allow this to be verified, but it is likely as atmosphere and temperature are highly variable inside a crucible. Therefore, the two types of slags can probably be linked to crucibles used during the same process.

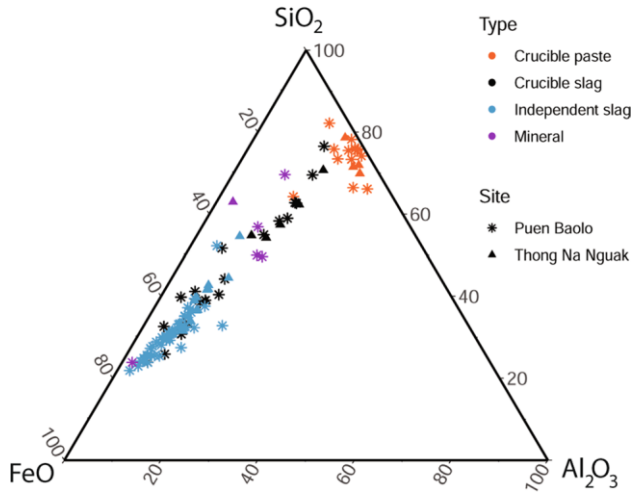

Figure 12 : Ternary diagram showing the average compositions in FeO, SiO2 and Al2O3 of the independent slags, the crucible slags, the minerals and the crucible paste for TNN and PBL (SEM–EDS, wt%)

The experimental smelts (Cadet et al. 2021) also raised questions: is it possible to obtain flat and homogeneous fayalitic slag by reduction in crucible, given it seems to require stable controlled conditions for its formation? The use of crucibles for one step of the metallurgical process also implies their association with a pit/hearth in which the crucible was placed for heating and also ventilation technologies such as tuyères (for which no remains were discovered). Different types of potential hearths were discovered at Puen Baolo. It can be assumed that some of these pits were used for metallurgical processes with a crucible, as their dimensions are consistent. Some pit features could correspond to different activities, potentially domestic, or changing practice over time but strata are too disturbed to allow such an interpretation.

Puen Baolo vs Thong Na Nguak

The Vilabouly Complex has two sites where production evidence could be investigated (at other sites, the upper layers were not identified early in the process and were removed by modern mining practices before they could be investigated archaeologically). Puen Baolo and Thong Na Nguak were compared and variations have been identified. Variations can be expressed through slag, particularly in manganese oxide and zinc oxide levels, which are higher for TNN. There is also a difference in metallic inclusions. Primary copper sulphides (chalcopyrite and bornite) are absent from TNN slags whereas they are commonly observed for PBL. However, it should also be noted that less archaeological material has been recovered from TNN which may induce a bias.

These two observations could indicate variation in raw materials used between the two sites, mainly ores, which in the case of TNN appear to be richer in manganese and zinc, the former of which can displace iron in the slag matrix. The co-smelting reduction mainly identified at PBL, does not seem to come into play in the same way at TNN.

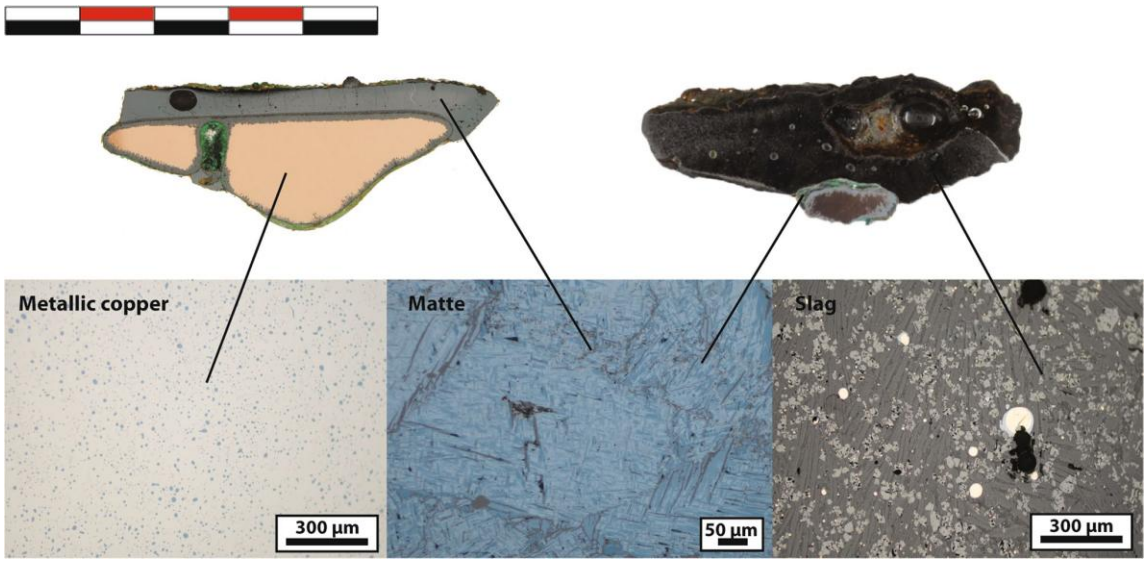

Figure 13 : OM images of the different layers identified for the multi-layered artefacts: metallic copper, matte and slag

Table 6 : SEM–EDS result for the different layers of the multi-layered artefacts: metallic copper, matte and slag

Matte	*O*	*Si*	*S*	*Fe*	*Cu*	*Al*						
SEALIP/LA/PBL/48	*3,0*	*0,1*	*22,0*	*1,0*	*74,0*	*0,0*						
SEALIP/LA/PBL/51	*3,5*	*0,0*	*23,5*	*1,0*	*72,0*	*0,0*						
SEALIP/LA/PBL/52	*8,0*	*1,0*	*17,0*	*1,5*	*71,5*	*0,6*						
SEALIP/LA/PBL/42	*8,0*	*0,1*	*23,0*	*0,2*	*68,5*	*0,0*						
Metallic Cu	*O*	*Si*	*S*	*Fe*	*Cu*	*As*						
SEALIP/LA/PBL/48	*2,0*	*0,0*	*1,5*	*0,2*	*96,5*	*0,0*						
SEALIP/LA/PBL/51	*0,7*	*0,0*	*0,1*	*1,0*	*97,5*	*0,6*						
SEALIP/LA/PBL/52	*0,9*	*0,0*	*1,0*	*0,1*	*98,0*	*0,0*						
SEALIP/LA/PBL/50	*0,8*	*0,4*	*1,0*	*0,0*	*97,5*	*0,3*						
Slag	*MgO*	*Al2O3*	*SiO2*	*P2O5*	*SO3*	*K2O*	*CaO*	*TiO2*	*MnO*	*FeO*	*CuO*	*ZnO*
SEALIP/LA/PBL/50	*0,7*	*6,0*	*30,0*	*0,5*	*0,2*	*1,0*	*1,0*	*0,7*	*2,0*	*55,0*	*2,0*	*0,3*
SEALIP/LA/PBL/51	*0,7*	*5,5*	*28,0*	*0,5*	*0,2*	*1,0*	*1,0*	*0,6*	*2,0*	*58,0*	*2,0*	*0,3*
BB14/3/3/7113	*0,0*	*5,0*	*27,0*	*0,0*	*0,0*	*0,0*	*4,0*	*0,0*	*0,0*	*63,0*	*0,9*	*0,0*
SEALIP/LA/PBL/49	*0,7*	*6,0*	*27,0*	*0,6*	*0,3*	*0,9*	*1,0*	*0,7*	*2,0*	*59,0*	*1,5*	*0,2*

Primary sulphides are absent from slag, which could mean two things: the presence of fewer sulphide ores in the TNN charge, or a process allowing better desulphurization. We have not been able to determine which is the case here as yet.
These variations in raw material are directly linked to different areas of copper mineralization in the VC. If we look again at the VC geology, the mineralizations at both

Khanong and Thengkham contain ‘exotic’ agglomerates of manganese copper. These agglomerates are sometimes associated with malachite, azurite, cuprite and native copper. They are found in the supergene zone disseminated in the first 25 m below surface. The presence of these exotic and shallow mineralizations with Cu-Mn ores may explain the higher presence of manganese oxide in TNN slags. The hypothesized difference between TNN and PBL ores is supported by the lead isotope data for the PBL and TNN ingots, in which a fine but significant, and consistent, variation appears (Cadet et al. 2019). This result could evidence VC mineralization exploitation varying over space (and potentially time), with a variable internal isotopic signature. The artefacts analyzed for TNN are few compared to PBL but all the analytical results seem to direct us towards a difference in mineral charge. The radiocarbon dates for TNN and PBL are of interest here. PBL (and the associated Thengkham South C mining shafts) evidences a significant Bronze Age (including likely *initial* Bronze Age) component, extending into the early and later Iron Age. On the other hand, dates from TNN (and the associated Khanong A2 mining shafts) span the early and middle Iron Age. Variation at PBL may represent early Bronze Age activity overlain and disturbed (mixed with) detritus from more expansive Iron Age processing activity.

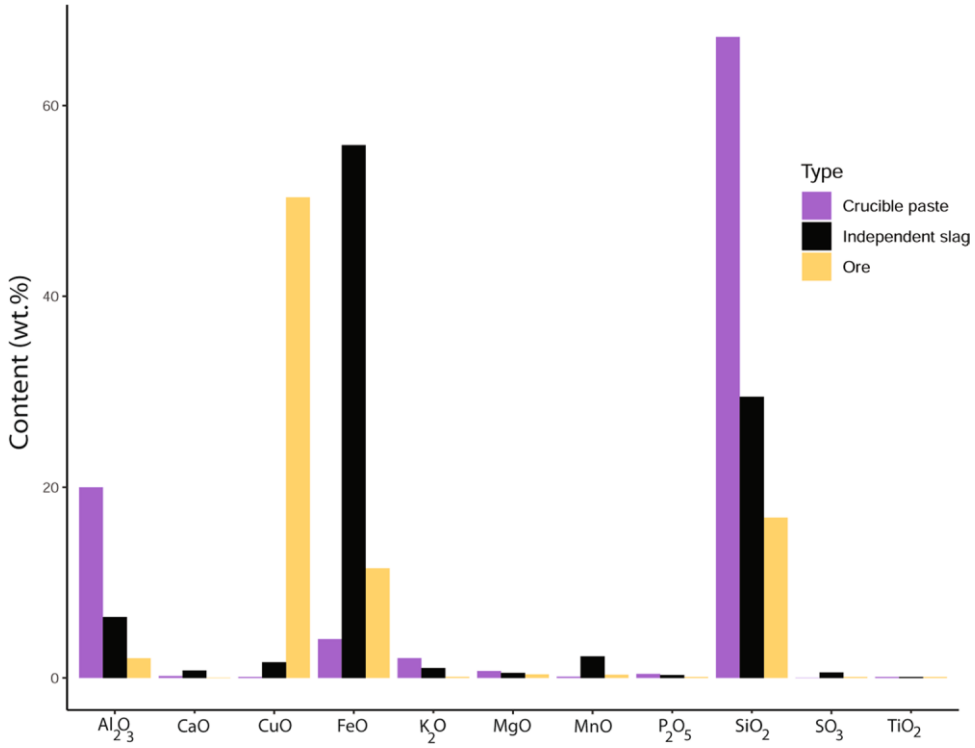

Figure 14 : Comparison of the average composition of oxides between the slags, the crucible paste and the ores (normalized data, wt%)

TNN merits further exploration, but excavations are impossible at this stage due to local beliefs and modern mining activity. In addition, the association of TNN with the Khanong A2 mining area, which has led to the discovery of numerous mining shafts, indicates large-scale mining activity. If the mining area of Khanong was indeed directly linked to the production activity of TNN, we can expect a much larger production site. TNN is potentially a complex, multi-component site with a swampy valley bottom associated with a level of open pit mining, and large areas of drier land.

The current data reflects the variations in copper mineralization between different areas of the VC. There could be two potential explanations of the variation between the PBL and TNN results. These are:

1. Two similar processes are being carried out at these sites, exploiting different raw materials and mineralizations. Thus, they would denote the parallel presence of at least two communities of artisans (given that we know of at least three other mining sites, there may be even more) exploiting different sites. Or,
2. The observed differences represent a temporal variation that has not yet been resolved. It is also possible that some combination of these two alternative explanations better represents the reality of the situation.

Vilabouly Complex copper production: comparison and integration at the scale of Mainland Southeast Asia

The radiometric and relative dating available for the Vilabouly Complex places its production activity from the turn of the 2nd/1st millennium BC until around the second half of the first millennium AD. VC production is now established to have begun at, or near the beginning of, the MSEA Bronze Age. If definite Bronze Age phases and samples were available, they would contribute to the discussion of technological transmissions from present-day China (Pigott and Ciarla 2007; White and Hamilton 2009; Higham et al. 2015, 2020; Pryce et al. 2018). VC's Bronze Age activity linked to copper artefacts is the first identified in all Laos, as the only other site with Bronze Age dating (one date) associated to a single copper-base artefact is the funerary context of Tam Pà Ling (Fig. 1) in northern Laos (Cameron et al. 2018; Pryce and Cadet 2018). Our corpus potentially incorporates these Bronze Age samples, but the low chronological resolution does not allow us to identify them. Only the so-called bowtie ingots (Cadet et al. 2019) identified in the lower-level graves of PBL, with copper dagger-axe *ge* (Chinese typology used from around 1600 BC and declined during the Han Period 206 BC–202 AD) and axes, have been associated with a Bronze Age context and may represent early extractive metallurgy at the VC. The bowtie shape, as well as bowl-shaped ingots (chance finds), have not been recorded elsewhere in prehistoric MSEA.

The VC data do not seem to show any traces of an experimental phase (cf. the KWPV, Pryce et al. 2010), but evidence an homogeneous production, which could be explained by copper metallurgy having arrived as a mature technology. The only significant difference is to be seen in the ingot typologies, with the lower level graves at Puen Baolo containing so-called bowtie ingots, and the upper level graves having conical ingots, in addition to iron objects. These two types of funerary contexts could then mean an evolution in the stylistic repertoire of the VC. Conical ingots may represent cultural, stylistic, change of the ingot's shape during the Iron Age and represents one of the few clear diachronic technological variations identified at PBL. Nothing so far shows a major evolution in the copper production processes themselves and thus supporting the hypothesis that metallurgy was introduce to the VC as a developed package, possibly by exogenous communities at a still undetermined period. The presence of objects bearing witness to exchanges with China and/or northern Vietnam, such as *ge* and *Dong Son* drums (Cadet et al. 2019), testifies at least to indirect contacts with relatively distant populations. The isotopic results also show potential indirect contacts with Thailand, Cambodia and as far as Myanmar (Pryce et al. 2011, 2014, 2016, 2017) since the Early Bronze Age (Myanmar/Thailand), as the VC signature has been identified in these regions. However, apart from Thailand, few data are available for these other regions

concerning copper metallurgical processes, which makes it difficult to discuss potential technological transfers between the different loci.

The three primary copper production centres currently known in MSEA (VC, Phu Lon and the Khao Wong Prachan Valley) seem to be involved in the same exchange networks (Pryce et al. 2011, 2014). Indeed, lead isotope data have revealed exchanges of raw materials (in two cases, PL/12 and NPW/1, potentially of minerals/slags,) between the three copper production centres. One might ask if these exchange networks only give rise to exchanges of objects/raw materials or if technological knowledge is also included. For the first time, the VC technological reconstruction can be compared with those of the KWPV (Bennett 1988a, b; Pryce 2008; Pryce et al. 2010) and Phu Lon (Pigott and Natapintu 1996; Vernon 1996; Pigott and Weisgerber 1998; Pryce et al.
2011; Pigott 2019) in Thailand as well as with secondary copper production centres.

Phu Lon seems to have been exploited for malachite ore but delivered very few artefacts linked to the primary copper production, maybe linked to the use of malachite, which can lead to a non-slagging process. Comparison with VC smelting processes is difficult given the few PL data available (only three slag samples were available to be analyzed, Pryce et al. 2011) but the shared use of crucibles and oxidic ores as well as relatively simple processes, are potentially notable.

The KWPV offers stronger evidence linking to the VC, with the use of co-smelting in crucibles to produce unalloyed copper ingots at multiple sites. One particular type of KWPV artefact illustrates these similarities: the multilayered artefacts named slag casts for KWPV (Pigott et al. 1997). The slag casts are described as slag which has solidified in a mould (Pryce 2008; Pryce et al. 2010). While the multi-layered artefacts from VC are composed of metallic copper, matte and/or slag, the KWPV slag casts are only composed of slag. It seems very likely that the slag casts could also have originally contained metallic copper or matte as with the examples from VC but, as these components had an economic value they have probably been re-used or reprocessed. In contrast, the artefacts from VC were discovered in a mortuary context. Similarly, copper ingots are likewise known from Iron Age KWPV graves, and 'Founder's burials' from Bronze Age phases.

Nevertheless, significant differences are observed in the quantity of material remains, which is much higher for the KWPV relative to the amount of slag recovered. This difference may be explained by the presence of more sulfidic ores and gangue minerals in the smelting charge at KWPV. As an aside, it is also worth noting that only some of the archaeological materials and sites have been discovered, and still less excavated, in the VC. Indeed, VC is still an active mining tenement. Most of the archaeological sites are on steep, mountainous land under dense forest, with the added complication that the area is heavily contaminated with unexploded ordinance from the Indo-China war periods (Jackson 2018). Despite key differences between VC and KWPV, the two production loci share common traits and could reveal a regional trend in prehistoric primary copper production. However, the production technologies remain simple and comparators can also be found in other parts of the world (Hauptmann et al. 2003; Nocete et al. 2008; Hanning et al. 2010; Erb-Satullo et al. 2015; Rehren et al. 2016). Rather than talking of 'technological transfers', it is equally possible that disparate Southeast Asian communities could have developed similar technological solutions, with local variants, linked to every context of production.

Another element common across these ancient MSEA copper production sites is crucibles. There appear to be different types for primary (larger) versus secondary (smaller, sometimes lagged and spouted) processes but the use of furnace structures remains very unclear at any

stage (Pryce et al. 2010). MSEA ancient crucibles appear small with a shallow-open form. In Thailand, a local lagging tradition has been identified in the northeast, for crucibles from Ban Chiang, Phu Lon and Ban Non Wat (Vernon 1996, 1997; Cawte 2012; Vernon et al. 2018) associated with secondary production. This lagging tradition has not been identified at VC, nor in the KWPV. Maybe the lagging tradition only comes into use during secondary production steps and represents a regional tradition present in northeast Thailand. Archaeological data revealed differences between primary production centres which are wider and mainly dedicated to the production of unalloyed copper, whereas secondary production sites are mostly settlement sites where other types of craft are practiced (iron smithing, pottery firing etc.). Furthermore, lead isotope data had revealed that some Thai sites such as Ban Chiang or Don Klang (Pryce 2019) were in part supplied by VC copper. One could imagine that artisans/communities travelled with VC copper, carrying with them some technological knowledge. Thus, while it is clear that VC metallurgy is part of the regional tradition as it has common features with other known sites, we have also revealed specificities and variants unique to the Vilabouly Complex, such as the Bronze Age bowtie and bowl-shaped ingots.

Furthermore, lead isotopic data for Bronze and Iron Age northern Vietnam have revealed no concordance with the VC so far (Pryce et al. 2014, 2022; Le Meur et al. 2021). This observation may suggest that northern Vietnam had access to different networks and copper supply, maybe in present-day China, that did not include the VC, despite the remarkably close geographical association. Importantly, VC is located close to a number of passes across the Truong Son Cordillera that separates the Mekong River from the Vietnamese coast. In terms of geography, at least, exchange to the east would be even more easy than the demonstrated relationships with locations to the west and south. Clearly, insufficient MSEA copper production sites have been identified yet and lead isotopic data are still lacking for some regions, especially from central and southern Vietnam, for definitive interpretations.

VC communities could be implanted in several spheres of interaction and parallel networks of exchanges (metal and glass) connecting Vietnam, central Laos, Thailand, Myanmar and Cambodia. These networks would have allowed the distribution of VC products, while contributing to the introduction of stylistic repertoires/non-regional objects, such as *ge*, *Dong son* drums and glass beads in central Laos. A potential communication route between the Iron Age *Sa Huynh* culture in central Vietnam, the Savannakhet plain in Laos and the Khorat Plateau (Thailand) has already been raised (Reinecke et al. 1999; Calo 2014) based on geography, as noted above, and historical precedent. The current major Lao Route 9 crosses from present day Mukdahan to the Vietnamese coast following this historical route. Some of the objects discovered at VC support the importance of this route, including the presence of *ge* and *dongson* drums. Non Nong Hor, a potential ancient production site of drums in Mukdahan province, has delivered conical ingots that look very similar to the multi-layered artefacts from VC (Baonoed 2016). This assumption needs to be verified by further studies but it's quite possible Non Nong Hor was supplied by VC copper and it might be interesting to explore the potential origin of the VC drums compared to Non Nong Hor. The likely jar burials at TNN also hint at an association with the jar burial tradition of the Vietnamese *Sa Huynh* culture (Dung 2001; Nishimura 2005; Higham 2014). Although it should be noted that there is no exact similarity at this stage and that most apparent mortuary contexts at VC reflect a different tradition. However, any contacts with the *Sa Huynh* culture could have permitted VC copper an indirect access to the maritime exchange networks and could partly

explain the distribution of its copper in Southeast Asia for sites situated far from Laos like Khao Sek in peninsular Thailand (Pryce and Bellina 2017).
Alternatively, the existence of a parallel inland 'Mekong Interaction Sphere' has also been proposed based on beads, ceramics and hard stone data (Carter 2015; Stark and Fehrenbach 2019; Carter et al. 2020). One of us (Chang) would argue that this is the more obvious interaction sphere represented by the finds, especially the Bronze Age mortuary traditions and associated personal ornaments, supported by lead isotopic data of Iron Age Cambodian sites consistent with the VC signature (Pryce et al. 2017). This Mekong Interaction Sphere would connect Iron Age VC with the territory of Fu Nan, other regions of Northern Cambodia and across central and northeastern Thailand and lowland Laos.
Finally, the clearly unique features of the Vilabouly Complex sites, including the ingot forms, but also aspects of the pottery (Cameron n.d.), the form of *ge* (Livingston 2014) and unique chalcedony beads (Eagleson 2019; A. Carter, pers. comm.) suggest that whatever exchange relationships the VC artisans were involved in, they also likely represented a unique and independent local identity.

Conclusion

Despite being at the heart of Mainland Southeast Asia, Laos is often absent, or little mentioned, from prehistoric regional syntheses. The present study's main aim is to better understand the Lao territory's and populations' roles during the prehistoric and early proto-historic periods. This was attempted by characterizing Vilabouly Complex primary copper production, the first such locale known in Laos and only the third regionally.
The various analytical datasets enabled us to propose a technological reconstruction of copper production, ranging from the extraction of minerals, smelting and casting. The results suggest a crucible-based reaction in a one-step smelting process, with a charge mainly composed of malachite and occasionally a mixture of ores (most likely malachite/chalcocite), depending on the mineralization being exploited. The ores used were relatively rich, leading to low quantities of slag production. The Vilabouly Complex seemed oriented towards the production of unalloyed copper, of which different types of potential ingots have been discovered (bowtie, conical and bowl). Technical or chronological variations were not observed except for ingots' shape. Indeed, the artefacts studied are a relatively homogeneous whole, suggesting little technological innovation over time. Differences were observed between the two most extensively investigated production sites of the Vilabouly Complex, Puen Baolo and Thong Na Nguak. Slag analysis and lead isotope data show variation in the raw materials used, which may relate to two different mineralization zones; Thengkham for Puen Baolo and Khanong for Thong Na Nguak. The data show exploitation, maybe by different settlements/artisans, of the two sites and/or different exploitation periods, though this cannot be proved with the current dating.
The VC production patterns share similar traits with other copper production centres in MSEA. The latter seem to be linked to a common evolution of practices (importantly, with local variations and choices) linked to adaptations conditioned by metallurgical practice (reduce, contain the metal, then cast it to obtain an object, obtain a practical shape for exchanges, etc.). Prehistoric sites were linked by numerous and parallel exchange networks that could transport VC copper to Thailand, Cambodia and Myanmar. This research leads to a variety of hypotheses concerning technological transfers and exchanges of copper with neighbouring regions; hypotheses that will lead to new projects exploring exactly how these early metallurgists were connected. In particular, this focuses us on the importance of better

understanding the exchange of knowledge and the level of integration of upland and land-locked populations with a wider technologically, culturally and economically diverse Mainland Southeast Asia through the early metal ages and into the early historic period.

Supplementary Information The online version contains supplementary material available at https://doi.org/10.1007/s12520-022-01608-0.

Acknowledgements We offer our thanks to the Lao Department of National Heritage who provided us help and permits in Laos for the initial recovery and export of the artefacts, along with the financial and logistical support of the mining concession operator MMG-LXML. This project would not have been possible without the support of the Vilabouly District communities and local government, Savannakhet Province cultural heritage officials and Archaeology staff and students of the National University of Laos and James Cook University. Many weeks, over several years, of hard physical work by representatives of all these institutions (in the context of a modern international commercial mining operation) lie behind this project. A special thanks to Eddy Foy who carried out the XRD analyses for the mineral samples at the LAPA. Also, thank you to the two anonymous reviewers for their comments which helped to improve this work. Special mention should be also made of Aj. Thongsa Sayavongkhamdy, the former director of the Lao Department of National Heritage who passed away early in 2022. His contribution to the archaeology & history of Laos, including this project, cannot be overstated. He will be long remembered.

Funding This work was financed by the French National Research ANR BROGLASEA 'Bronze and Glass as Cultural Catalysts and Tracers in Early Southeast Asia' (ANR-16-CE27-0011), directed by T.O. Pryce.

References

Addis A, Angelini I, Artioli G (2017) Late Bronze Age copper smelting in the southeastern Alps: how standardized was the smelting process? Evidence from Transacqua and Segonzano, Trentino, Italy. Archaeol Anthropol Sci 9:985–999. https://doi.org/10.1007/s12520-016-0462-5

Addis A, Angelini I, Nimis P, Artioli G (2016) Late Bronze Age copper smelting slags from Luserna (Trentino, Italy): interpretation of the metallurgical process. Archaeometry 58:96–114. https://doi.org/ 10.1111/arcm.12160

Bachmann HG (1982) The identification of slags from archaeological sites. Institute of Archaeology, London

Baonoed S (2016) Non Nong Hor: the production site of bronze drum in Thailand. In: Abstracts of The 2nd SEAMEO SPAFA International Conference on Southeast Asian archaeology, 30th May-2nd June. Bangkok

Bayley J, Rehren T (2007) Towards a functional and typological classification of crucibles. In: La Niece S, Hook D, Craddock PT (eds) Metals and mines: studies in archaeometallurgy. Archetype book, pp 46–55

Bennett A (1988a) Prehistoric copper smelting in Central Thailand. In: Charoenwongsa, Bronson B (eds) Prehistoric studies: the stone and metal ages in Thailand. Bangkok, pp 125–135

Bennett A (1988b) Copper metallurgy in Central Thailand. Unpublished doctoral thesis. Institute of Archaeology, University College London

Bourdonneau E (2003) The ancient canal system of the Mekong Delta preliminary report. In: Källen A, Karlström A (eds) Fishbones and glittering emblems. Southeast Asia Archaeology 2002. Museum of Far Eastern Antiquities, pp 257–270
Bourdonneau E (2005) Indianisation et formation de l'État en Asie du Sud-Est : Retour sur trente ans d'historiographie . Matériaux pour l'étude du Cambodge ancien. Unpublished docoral thesis. Université Paris I
Bourgarit D, Rostan P, Carozza L et al (2010) Vingt ans de recherches à Saint-Véran, Hautes Alpes: état des connaissances de l'activité de production de cuivre à l'âge du Bronze ancien. Trab Prehist 67:269–285. https://doi.org/10.3989/tp.2010.10039
Burger E (2008) Métallurgie extractive protohistorique du cuivre :Etude thermodynamique et cinétique des réactions chimiques de transformation de minerais de cuivre sulfurés en métal et caractérisation des procédés. Unpublished doctoral thesis. Université Pierre et Marie Curie Paris VI
Cadet M, Sayavongkhamdy T, Souksavatdy V et al (2019) Laos' central role in Southeast Asian copper exchange networks: a multimethod study of bronzes from the Vilabouly Complex. J Archaeol Sci 109:104988. https://doi.org/10.1016/j.jas.2019.104988
Cadet M, Tereygeol F, Sayavongkhamdy T et al (2021) Late prehistoric copper smelting in the Lao PDR: experimental reconstruction based on the Vilabouly Complex evidence. J Archaeol Sci Rep 37.https://doi.org/10.1016/j.jasrep.2021.102932
Calo A (2014) Trails of Bronze Age drums across early Southeast Asia: exchange routes and connected cultural spheres. Institute of Southeast Asian Studies, Singapore
Cameron K (n.d.) Pottery production and society in an ancient mining community in Laos. Unpublished doctoral thesis. James Cook University
Cameron K, Chang N, Ravenscroft M (2018) Le mobilier de la sépulture de Tam Pà Ping: révélateur d'une pratique funéraire de la transition Néolithique/Age du Bronze dans les Hautes Terres du Laos. In: Patole-Edoumba E, Demeter F (eds) Pà Hang, la montagne habitée: 100000 ans d'histoire de la biodiversité et de l'occupation humaine au nord du Laos. Les Indes savantesMuseum d'Histoire Naturelle de la Rochelle, La Rochelle, pp 171–196
Carignan J, Hild P, Mevelle G et al (2001) Routine analyses of trace elements in geological samples using flow injection and low pressure on line liquid chromatography coupled to ICP-MS: a study of geochemical reference material BR, DR-N, EB-N, AN-G and GH. Geostand Newsl 25:187–198
Carratoni L, Meucci C, Rispoli F (2018) Ceramics from prehistoric Non Pa Wai, Central Thailand: a preliminary petrographic investigation. Archaeol Res Asia 16:116–129. https://doi.org/10.1016/j. ara.2018.07.001
Carter AK (2015) Beads, exchange networks and emerging complexity: a case study from Cambodia and Thailand (500 BCE-CE 500). Camb Archaeol J 25:733–757
Carter AK, Dussubieux L, Stark MT, Gilg HA (2020) Angkor Borei and protohistoric trade networks: a view from the glass and stone bead assemblage. Asian Perspect 60:32–70. https://doi.org/10. 1353/asi.2020.0036
Cawte H (2012) The crucibles and moulds. In: Higham CF, Kijngam A (eds) The origins of the civilization of Angkor: Volume 5: the excavation of Ban Non Wat: the Bronze Age. Fine Art Department of Thailand, Bangkok, pp 458–486
Chang N (2016) Archaeology on the MMG-LXML Sepon Operation tenement (Vilabouly District, Savannakhet Province, Laos). Unpublished report. James Cook University

Cromie PW (2010) Geological setting, geochemistry and genesis of the Sepon gold and copper deposits, Laos. Unpublished doctoral thesis. Centre of Excellence in Ore Deposits University of Tasmania
Cromie P, Makoundi C, Zaw K et al (2018) Geochemistry of Au-bearing pyrite from the Sepon Mineral District, Laos DPR, Southeast Asia: implications for ore genesis. J Asian Earth Sci 164:194–218. https://doi.org/10.1016/j.jseaes.2018.06.014
Dung LTM (2001) Exogenous and indigenous factors in the formation of early states in Central Vietnam. Cham Stud 2:51–61
Eagleson T (2019) A study of precious stone beads from Savannakhet Province, Vilabouly, Laos. Unpublished BA (Hons) Dissertation. James Cook University
Edmonds M (1990) Description, understanding and the chaîne operatoire. Archaeol Rev Camb 9:55–70
Erb-Satullo NL, Gilmour BJJ, Khakhutaishvili N (2015) Crucible technologies in the Late Bronze-Early Iron Age South Caucasus: copper processing, tin bronze production, and the possibility of local tin ores. J Archaeol Sci 61:260–276. https://doi.org/10.1016/j.jas.2015.05.010
Georgakopoulou M, Bassiakos Y, Philaniotou O (2011) Seriphos surfaces: a study of copper slag heaps and copper sources in the context of early bronze age aegean metal production. Archaeometry 53:123–145. https://doi.org/10.1111/j.1475-4754.2010.00529.x
Glover IC, Yamagata M (1995) The origins of the Cham civilization: indigenous, Chinese and Indian influences in Central Vietnam by excavations at Tra Kieu, Vietnam 1990 and 1993. In: Young C, Li W (eds) Archaeology of Southeast Asia. University Museum Art and Gallery, Hong Kong
Grazulis S, Chateigner D, Downs R et al (2009) Crystallography open database an open-access collection of crystal structures. J Appl Crystallogr 42:726–729
Hammersley AP, Svensson SO, Hanfland M et al (1996) Two-dimensional detector software: from real detector to idealised image or two-theta scan. High Press Res 14:235–248
Hanning E, Gauß R, Goldenberg G (2010) Metal for Zambujal: experimentally reconstructing a 5000-year-old technology. Trab Prehist 67:287–304.
https://doi.org/10.3989/tp.2010.10040
Hauptmann A (2007) The archaeometallurgy of copper evidence from Faynan, Jordan. Springer Verlag, Heidelberg
Hauptmann A, Rehren T, Schmitt-Strecker S (2003) Early Bronze Age copper metallurgy at Shahr-i Sokhta (Iran), reconsidered. In: Stöllner T, Körlin G, Steffens G, Cierny J (eds) Man and mining. Deutsch Bergbau-Museum, Bochum, pp 197–213
Herdits H (2003) Bronze Age smelting site in the Mitterberg mining area in Austria. In: Craddock PT, Lang J (eds) Mining and metal production through the ages. British Museum Press, London, pp 69–75
Higham CF (2014) Early Mainland Southeast Asia : from first humans to Angkor. River Book, Bangkok
Higham CF, Douka K, Higham T (2015) A new chronology for the bronze age of northeastern Thailand and its implications for Southeast Asian prehistory. PLoS ONE 10:1–20.
https://doi.org/ 10.1371/journal.pone.0137542
Higham T, Weiss A, Pigott VC et al (2020) A prehistoric copper-production centre in Central Thailand: its dating and wider implications. Antiquity 94:948–965
Jackson R (2018) Migration to two mines in Laos. Sustain Dev 26:471–480
Karlström A, Källen A (1997) Lao Pako archaeological excavation 1995. Unpublished report

Kresten P (1986) Melting points and viscosities of ancient slags: a discussion. Hist Metall 20:43–45
Larreina-García D (2017) Copper and bloomery iron smelting in Central China Technological traditions in the Daye County (Hubei). Unpublished doctoral thesis. University College London
Le Meur C, Cadet M, Van Doan N et al (2021) Typo-technological, elemental and lead isotopic characterization and interpretation of Đông Sơn miniature drums. J Archaeol Sci Rep 38.https://doi.org/ 10.1016/j.jasrep.2021.103017
Livingston C (2014) Who were the people of ancient Vilabouly? Exploring origins and relationships through the study of Ge. James Cook University, Townsville
Lorrillard M (2014) Pre-Angkorian communities in the Middle Mekong Valley (Laos and adjacent areas). In: Revire N, Murphy SA (eds) Before Siam: essays in art and archaeology. River Book, Bangkok, pp 187–215
Malleret L (1959) L'Archéologie du Delta du Mekong, vol 4. EFEO, Paris
Manguin P-Y (2009) The archaeology of Funan in the Mekong River delta: the "Oc Eo culture" of Vietnam. In: Tingley N, Reinecke A, Manguin P-Y (eds) Arts of ancient Viet Nam: from river plain to open sea, Art Societ. Museum of Fine Arts, pp 100–118
Manini T, Aquino J, Gregory C, Aneka S (2001) Discovery of the Sepon District gold and copper deposits, Laos. Unpublished report for Oxiana Resources. Perth
Metten B (2003) Beitrag zur spätbronzezeitlichen Kupfermetallurgie im Trentino (Südalpen) im Vergleich mit anderen prähistorischen Kupferschlacken aus dem Alpenraum. Metalla 10:1–122
Nishimura M (2005) Chronology of the metal age in the Southern Vietnam. JSAA 25
Nocete F, Queipo G, Sáez R et al (2008) The smelting quarter of Valencina de la Concepción (Seville, Spain): the specialised copper industry in a political centre of the Guadalquivir Valley during the Third millennium BC (2750–2500 BC). J Archaeol Sci 35:717–732. https://doi.org/10.1016/j.jas.2007.05.019
O'Reilly D, Shewan L, Domett K et al (2019) Excavating among the megaliths: recent research at the 'Plain of Jars' site 1 in Laos. Antiquity 93:970–989. https://doi.org/10.15184/aqy.2019.102
Pigott VC (2019) Prehistoric copper mining and smelting in Southeast Asia: evidence from Thailand and Laos. In: White JC, Hamilton EG (eds) Ban Chiang, Northeast Thailand, volume 2C: the metal remains in regional context. University of Pennsylvania Museum of Archaeology and Anthropology, Philadelphia, pp 5–57
Pigott VC, Ciarla R (2007) On the origins of metallurgy in prehistoric Southeast Asia: the view from Thailand. In: La Niece S, Hook DR, Craddock PT (eds) Metals and mines – studies in archaeometallurgy. London Archetype Publication
Pigott VC, Natapintu S (1996) Investigating the origins of metal use in prehistoric Thailand. In: Bulbeck FD, Bernard N (eds) Ancient Chinese and Southeast Asian Bronze Age cultures. The proceedings of a Conference held at the Edith and Joy London Foundation Property, Kioloa, NSW. 8–12 February, 1988. SMC publishing, Taipei, pp 787–808
Pigott VC, Weisgerber G (1998) Mining archaeology in geological context. The prehistoric copper mining complex at Phu Lon, Nong Khai Province, northeast Thailand. In: Rehren T, Hauptmann A, Mulhy JD (eds) Metallurgica antiqua: in honour of Hans-Gert Bachmann and Robert Maddin. Deutsche Bergbau-Museum Bochum, pp 135–161
Pigott VC, Weiss AD, Natapintu S (1997) The archaeology of copper production: excavations in the Khao Wong Prachan Valley, Central Thailand. In: Ciarla R, Rispoli F (eds) South-East

Asian Archaeology, 1992. Proceedings of the Fourth International Conference of the European Association of South-East Archaeologists. Rome, 28th September-4th October 1992. Serie Orientale Roma Vo. 77, Instituto Italiano per l'Africa e l'Oriente, Rome, pp 119–157
Pryce TO (2008) Prehistoric copper production and technological reproduction in the Khao Wong Prachan Valley of Central Thailand. Unpublished doctoral thesis. Institute of Archaeology, University College London
Pryce TO (2013) Sedentary and metallurgy in upland Southeast Asia. In: Evrard O, Guililaud D, Vaddhanaphuti C (eds) Mobility and heritage in Northern Thailand and Laos: past and present Proceedings of the Chiang Mai Conference, 1–2 December 2011. pp 27–45
Pryce TO (2019) Lead isotope characterization and provenance of copper-base artifacts from Ban Chiang and Don Klang. In: White JC, Hamilton EG (eds) Ban Chiang, Northeast Thailand, volume 2C: the metal remains in regional context. University of Pennsylvania Museum of Archaeology and Anthropology, Philadelphia, pp 57–64
Pryce TO, Bellina B (2017) High-tin bronze bowls and copper drums: non-ferrous archaeometallurgical evidence for Khao Sek's involvement and role in regional exchange systems. Archaeol Res Asia 13:50–58. https://doi.org/10.1016/j.ara.2017.07.002
Pryce TO, Cadet M (2018) Métallurgie du cuivre ancienne au Lao PDR. In: Patole-Edoumba E, Demeter F (eds) Pà Hang, la montagne habitée: 100000 ans d'histoire de la biodiversité et de l'occupation humaine au nord du Laos. Les Indes savantes-Museum d'Histoire Naturelle de la Rochelle, La Rochelle, pp 196–206
Pryce TO, Baron S, Bellina B et al (2014) More questions than answers: the Southeast Asian Lead Isotope Project 2009–2012. J Archaeol Sci 42:273–294. https://doi.org/10.1016/j.jas.2013.08.024
Pryce TO, Brauns M, Chang N et al (2011) Isotopic and technological variation in prehistoric Southeast Asian primary copper production. J Archaeol Sci 38:3309–3322. https://doi.org/10.1016/j.jas. 2011.07.016
Pryce TO, Cadet M, Allard F et al (2022) Copper-base metal supply during the northern Vietnamese Bronze and Iron Ages: metallographic, elemental, and lead isotope data from Dai Trach, Thành Dên, Gò Mun, and Xuân Lâp. Archaeol Anthropol Sci 14.https:// doi.org/10.1007/s12520-021-01489-9
Pryce TO, Htwe KMM, Georgakopoulou M et al (2016) Metallurgical traditions and metal exchange networks in late prehistoric central Myanmar, c. 1000 BC to c. AD 500. Archaeol Anthropol Sci 10:1087–1109. https://doi.org/10.1007/s12520-016-0436-7
Pryce TO, O'Reilly D, Shewan L (2017) Copper-base metallurgy in Late Iron Age Cambodia: evidence from Lovea. J Archaeol Sci Rep 13:395–402. https://doi.org/10.1016/j.jasrep.2017.04.005
Pryce TO, Kyaw AA, Kyaw MM, Win TT (2018) A first absolute chronology for Late Neolithic to Early Bronze Age Myanmar: new AMS 14C dates from Nyaung'gan and Oakaie. Antiquity 92:690–708
Pryce TO, Pigott VC, Martinón-Torres M, Rehren T (2010) Prehistoric copper production and technological reproduction in the Khao Wong Prachan Valley of Central Thailand. Archaeol Anthropol Sci 2:237–264. https://doi.org/10.1007/s12520-010-0043-y
Rademakers FW (2015) Into the crucible: methodological approaches to reconstructing crucible metallurgy, from New Kingdom Egypt to Late Roman Thrace. Unpublished doctoral thesis. UCL London

Rademakers FW, Rehren T (2016) Seeing the forest for the trees: assessing technological variability in ancient metallurgical crucible assemblages. J Archaeol Sci Rep 7:588–596. https://doi.org/ 10.1016/j.jasrep.2015.08.013
Rehren T (2003) Crucibles as reaction vessels in ancient metallurgy. In: Craddock P, Lang J (eds) Mining and metal production through the ages. British Museum Press, London, pp 207–215
Rehren T, Boscher L, Pernicka E (2012) Large scale smelting of speiss and arsenical copper at Early Bronze Age Arisman, Iran. J Archaeol Sci 39:1717–1727. https://doi.org/10.1016/j.jas.2012.01.009
Rehren T, Charlton M, Chirikure S et al (2007) Decisions set in slag: the human factor in African iron smelting. In: La Niece S, Hook DR, Craddock PT (eds) Metal and mines-studies in archaeometallurgy. Archetype Publication, London, pp 211–218
Rehren T, Leshtakov P, Penkova P (2016) Reconstructing Chalcolithic copper smelting at Akladi Cheiri. In: Nilokov V, Schier W (eds) Der Schwarzmeerraum vom Neolithikum bis in die Früheisenzeit (6000–600 v.Chr.). Alle Rechte vorbehalten, pp 205–214
Reinecke A, Son LD, Phuc LD (1999) Towards a prehistory in the northern part of central Vietnam. A review following a Vietnamese-German research project. In: Beiträge zur allgemeinen und vergleichenden archäologie. Kommission für Allgemeine und Vergleichende Archäologie des Deutschen Archäologischen Instituts, Bonn, pp 5–59
Rostoker W, Dvorak JR (1991) Some experiments with co-smelting to copper alloys. Archeomaterials 5:5–20
Rostoker W, Pigott VC, Dvorak JR (1989) Direct reduction to copper metal by oxide-sulfide mineral interaction. Archeomaterials 3:69–87
Sillitoe RH (1998) Comments on geology and exploration potential for copper and gold deposits at Sepon, Laos. A Rep Prep Lane Xang Miner Ltd
Stark MT (1998) The transition to history in the Mekong Delta: a view from Cambodia. Int J Hist Archaeol 2:175–204
Stark MT (2015) Inscribing legitimacy and building power in the Mekong Delta. In: Emberling G (ed) Social theory in archaeology and ancient history: the present and futur of counternarratives. Cambridge University Press, Cambridge, pp 75–106
Stark MT, Fehrenbach S (2019) Earthenware ceramic technologies of Angkor Borei, Cambodia. Udaya J Khmer Stud:109–135
Tomber R, Cartwright C, Gupta S (2011) Rice temper: technological solutions and source identification in the Indian Ocean. J Archaeol Sci 38:360–366. https://doi.org/10.1016/j.jas.2010. 09.014
Tucci A, Sayavongkhamdy T, Chang N, Souksavatdy V (2014) Ancient copper mining in Laos: heterarchies, incipient states or post-state anarchists? J Anthropol Archaeol 2:1–15. https://doi.org/10. 15640/jaa.v2n2a1
Vernon WW (1996) The crucible in copper-bronze production at prehistoric Phu Lon, northeast Thailand: analyses and interpretation. In: Bulbeck FD, Barnard N (eds) Ancient Chinese and Southern Asian Bronze cultures 1988. SMC publishing, Taipei, pp 809–820
Vernon WW (1997) Chronological variation in crucible technology at Ban Chiang: a preliminary assessment. Bull Indo-Pacific Prehist Assoc 16:107–110
Vernon WW, White JC, Hamilton EG (2018) Metal product manufacturing evidence: crucibles, molds and slags. In: White JC, Hamilton EG (eds) Ban Chiang, Northeast Thailand, volume 2B: metals and related evidence from Ban Chiang, Ban Tong, Ban Phak Top, and Don Klang. University of Pennsylvania press, Philadelphia, pp 103–124

Vincent B (2003) Rice in pottery: new evidence for early rice cultivation in Thailand. Indo Pac Prehist Assoc Bull 23:51–58
White JC, Hamilton EG (2009) The transmission of Early Bronze technology to Thailand: new perspectives. J World Prehist 22:357– 397. https://doi.org/10.1007/s10963-009-9029-z
White JC, Lewis H, Bouasisengpaseuth B et al (2009) Archaeological investigations in northern Laos: contributions to Southeast Asian prehistory. Antiquity 83 (online